南京航空航天大學
NANJING UNIVERSITY OF AERONAUTICS AND ASTRONAUTICS

材料科学与技术学院
COLLEGE OF MATERIALS SCIENCE AND TECHNOLOGY

# Structure study of light superheavy nuclei by PNC-CSM method

**Xiao-Tao He**

Nanjing University of Aeronautics and Astronautics (NUAA)

Collaborators: Jun Zhang,Yu-Chun Li, Shu-Yong Zhao, Yi-Fei Xu (NUAA),
Zhen-Hua Zhang (NCEPU),
Zhong-Zhou Ren (TJU),
Shan-Gui Zhou, En-Guang Zhao (ITP,CAS)

CWAN’23, Chirality and Wobbling in Atomic Nuclei July 10 - July 14, 2023, Huizhou, China

# Outline

1. Introduction
2. Theoretical Framework of PNC-CSM
3. Results and discussions
4. Summary

# 1. Introduction

# 1.1 Why Transfermium nuclei?

**Tansfermium nuclei（Z ≥ 100）：** the **heaviest** system accessible in present in-beam experiment.

**Way to get structure information about very heavy nuclear system：**

- ✓ ***α*-decays:** life time, spin, parity … …
- ✓ **Spectroscopy of collective rotation:** spin, parity, configurations, deformations, single-particle orbital … …

☐ **Study of the spectroscopy of the nuclei with Z ~ 100 provide an indirect way to access the single particle states of the next closed spherical shells.**

# 1.1 Why Transfermium nuclei?

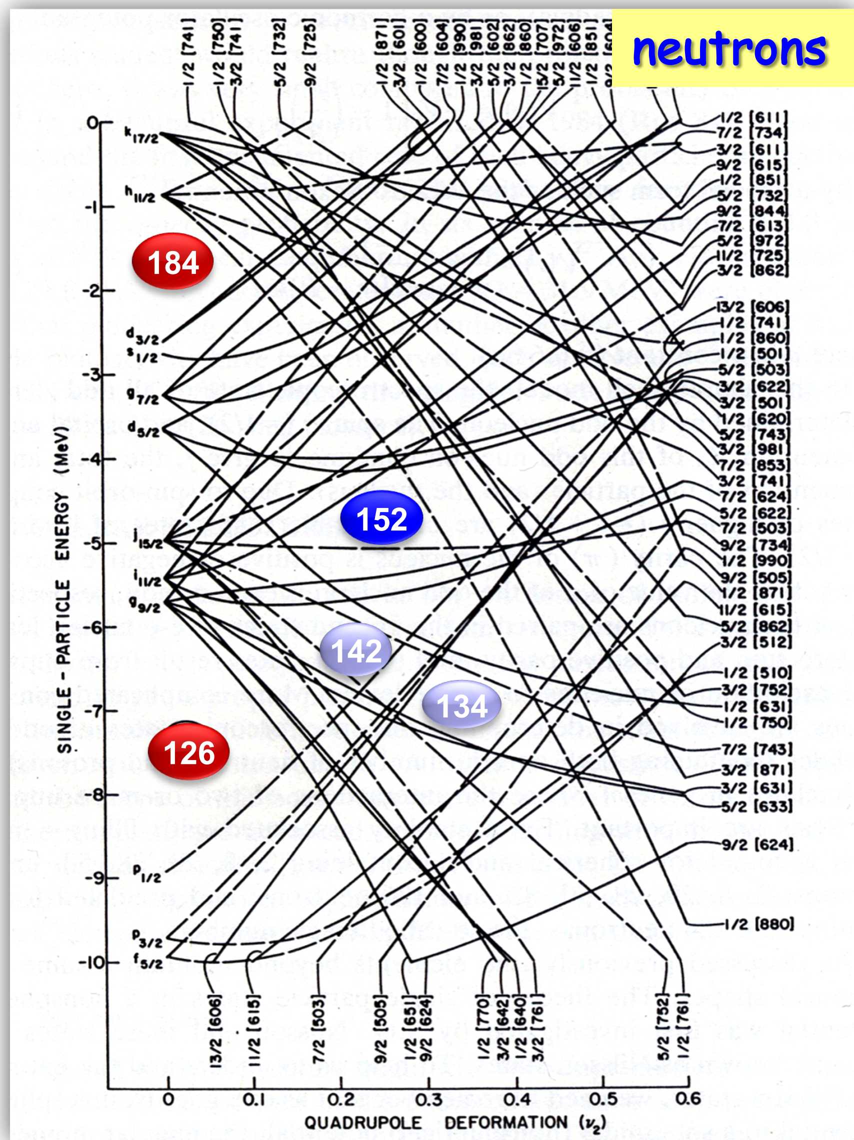


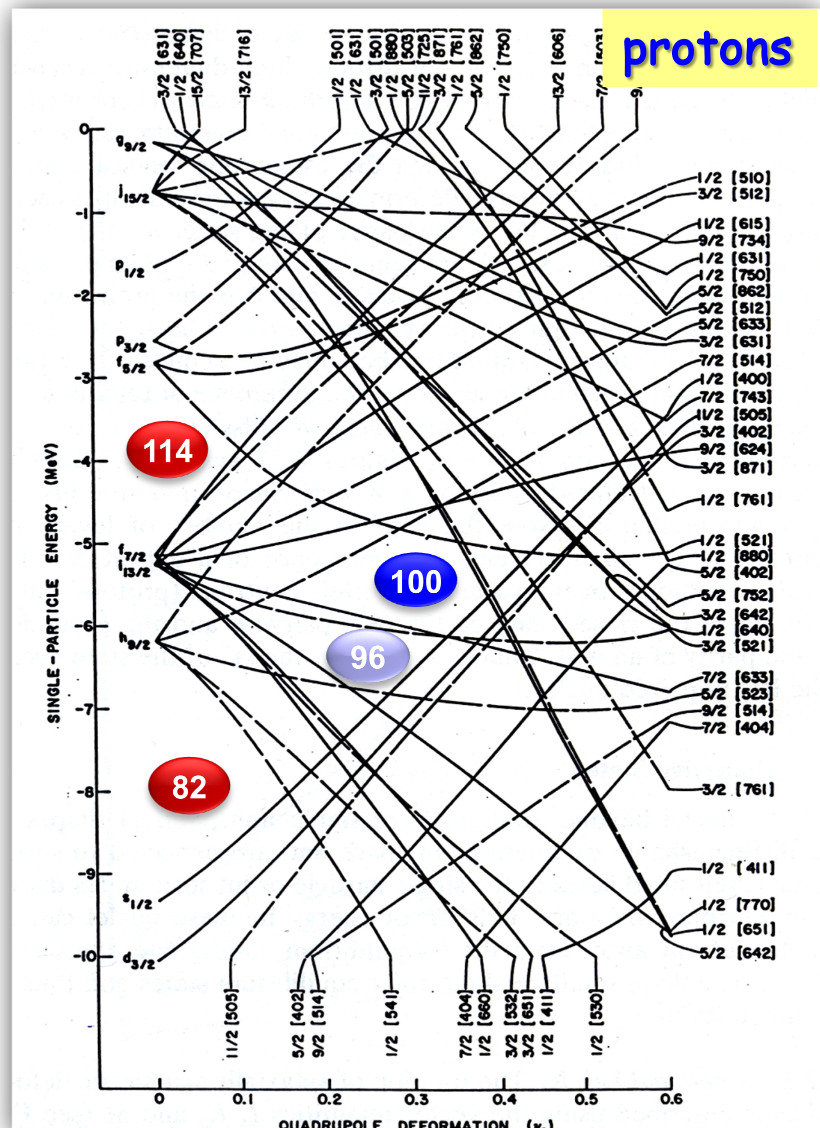


**Diagrams for Neutron (left) and proton (right) single particle levels - Woods-Saxon potential**

# 1.1 Why Transfermium nuclei?

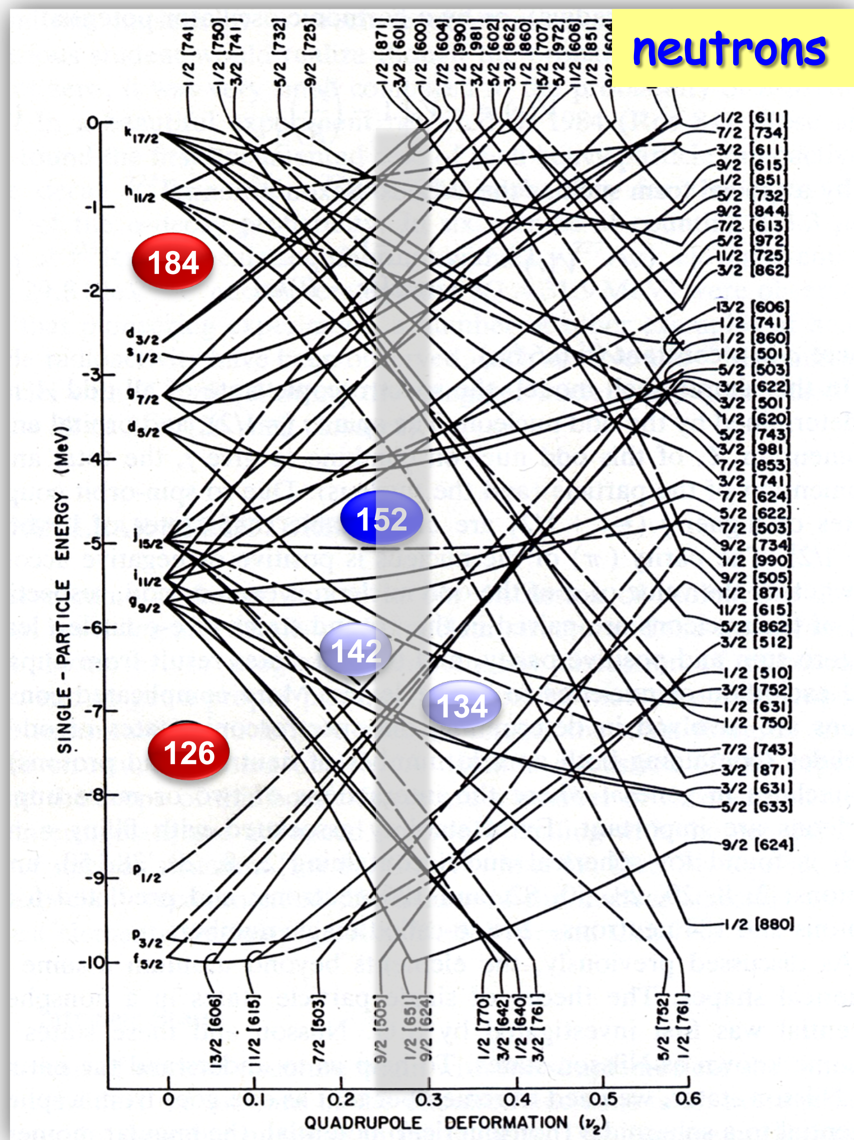


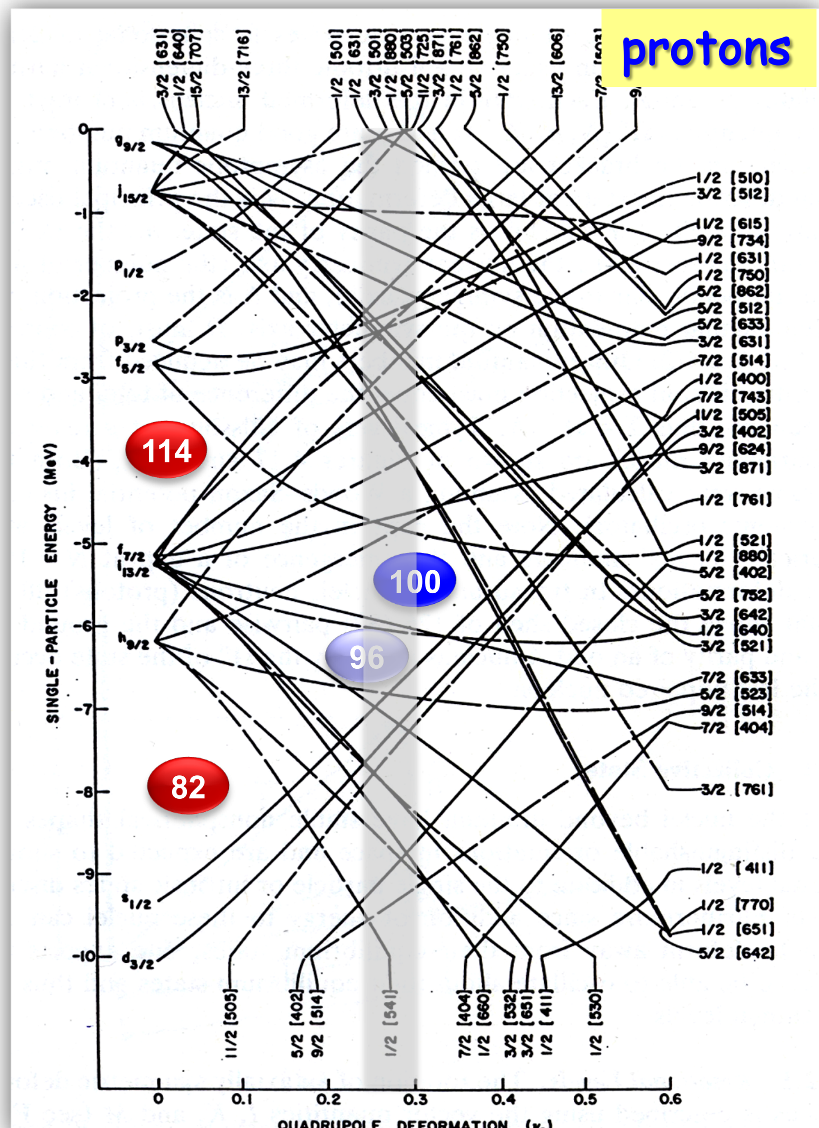


**Diagrams for Neutron (left) and proton (right) single particle levels - Woods-Saxon potential**

# 1.1 Why Transfermium nuclei?

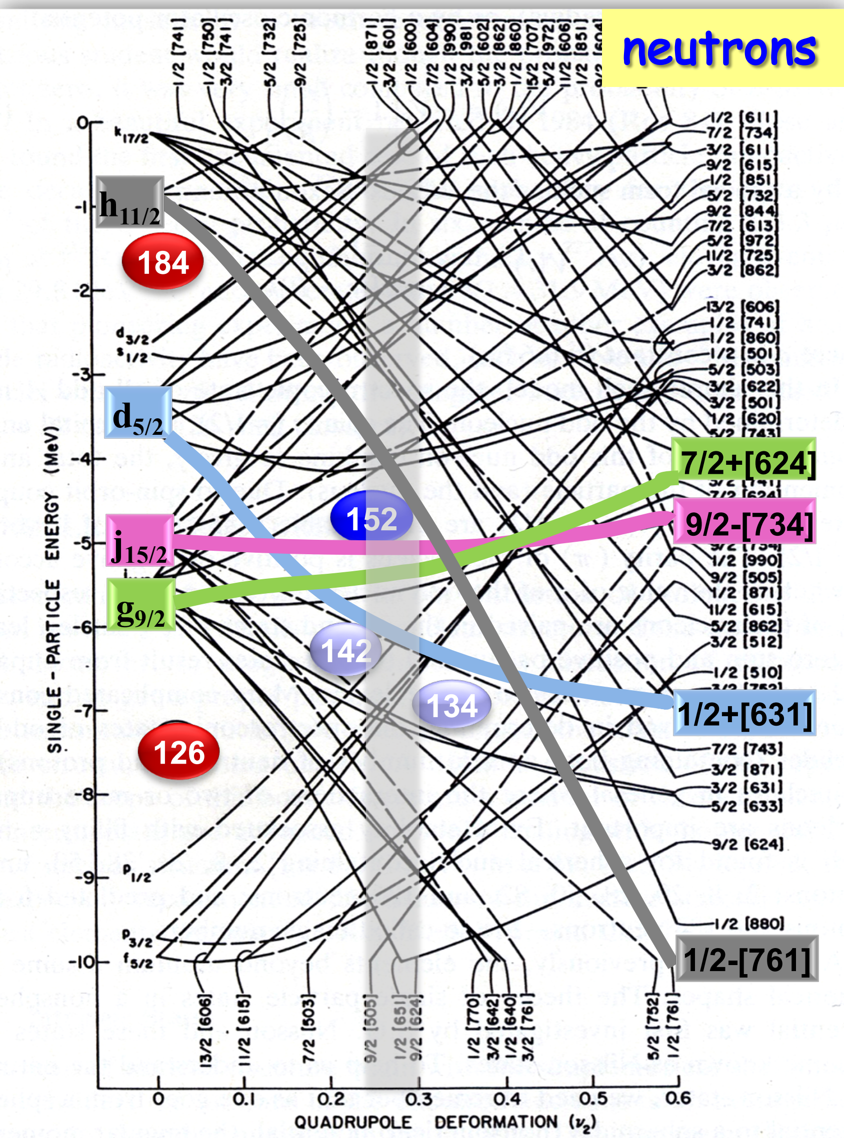


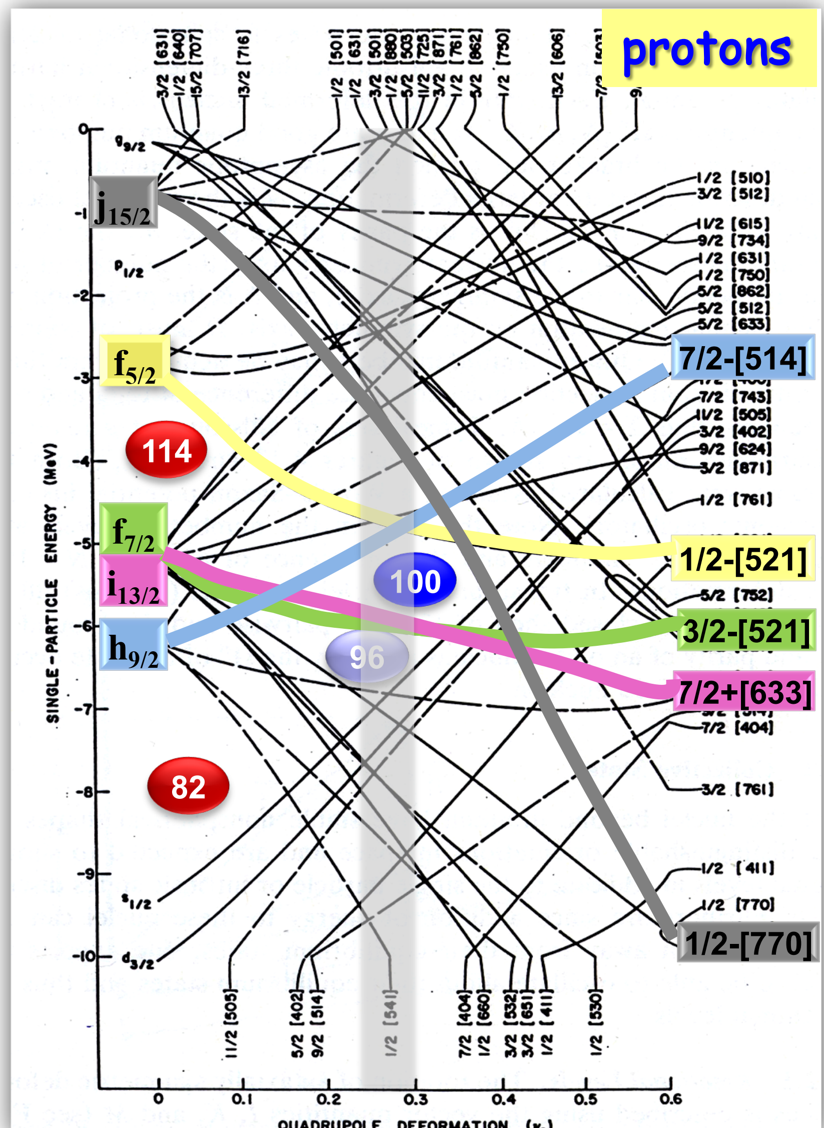


**Diagrams for Neutron (left) and proton (right) single particle levels - Woods-Saxon potential**

# 1.2 Known data→ Rotational spectroscopy

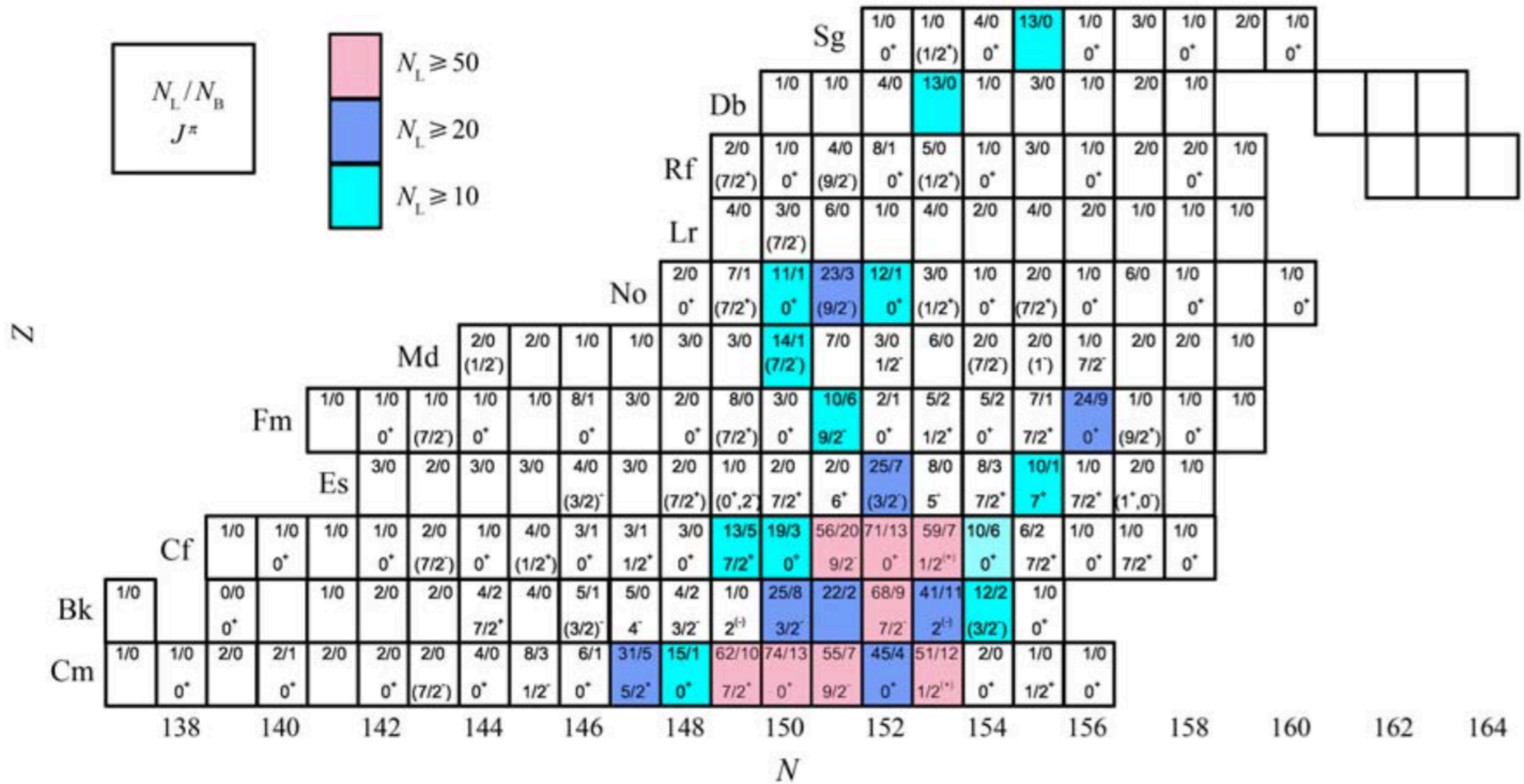


图 1　(在线彩图) 质子数 Z = 96 (Cm) 到 106 (Sg) 的原子核谱学实验数据统计

Zhang Zhenhua, Wen Kai, **HXT**, Zeng Jinyan, Zhao Enguang, Zhou Shangui, Nuclear Physics Review 30 (2013) 268.

# 1.2 Known data→ High-K isomer

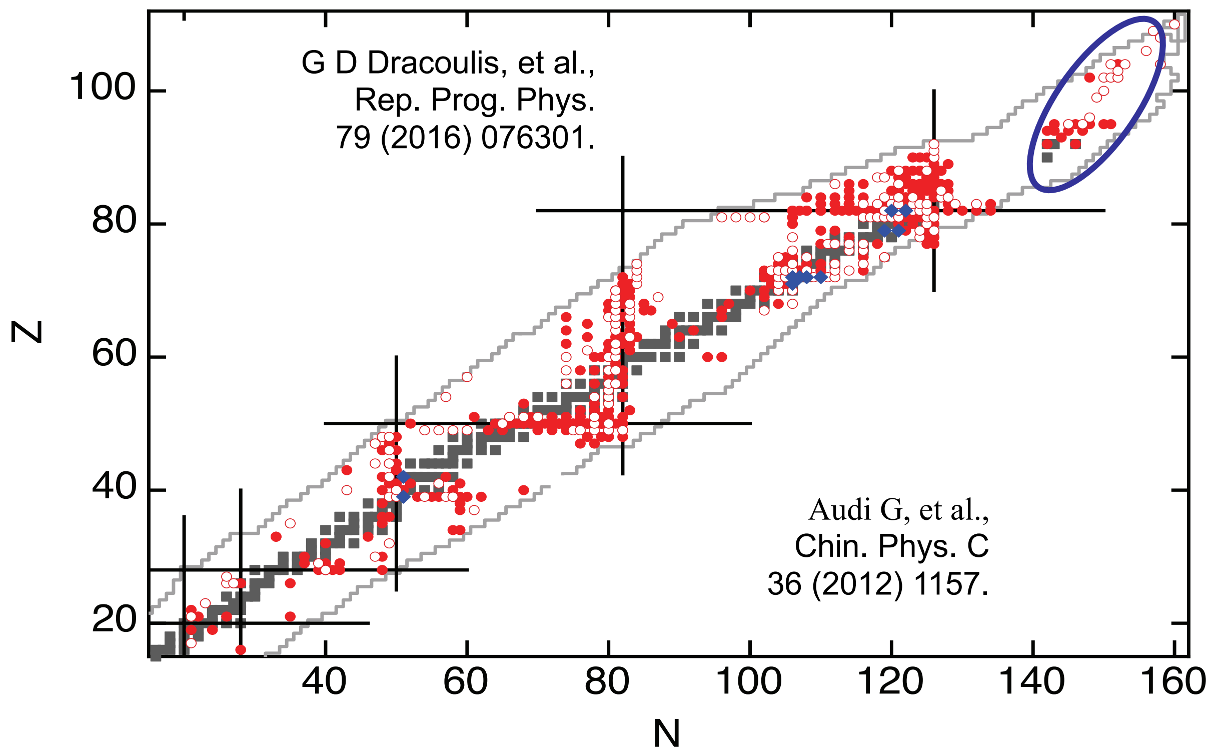


**Figure 1.** Nuclear chart illustrating the distribution of isomers with excitation energies greater than 600 keV, with data from Audi *et al* [44]. The filled red circles correspond to 200 ns $< T_{1/2} <$ 100 $\mu$s, the open red circles correspond to 100 $\mu$s $< T_{1/2} <$ 1 h, and the filled blue diamonds are for $T_{1/2} >$ 1 h.

# 2. Theoretical Framework

# 2.1 Theoretical framework of PNC-CSM

## Cranked Shell Model (CSM) Hamiltonian:

$$
\begin{aligned}
H_{\mathrm{CSM}} &= H_{\mathrm{SP}} - \omega J_x + H_{\mathrm{P}}(0) + H_{\mathrm{P}}(2) \\
&= \underline{\sum_{\xi} h_\xi - \omega J_x} - \underline{G_0 \sum_{\xi\eta} a_\xi^\dagger a_{\bar{\xi}}^\dagger a_{\bar{\eta}} a_\eta - G_2 \sum_{\xi\eta} q_2(\xi) q_2(\eta) a_\xi^\dagger a_{\bar{\xi}}^\dagger a_{\bar{\eta}} a_\eta} \ ,
\end{aligned}
$$

1. $h_0(\omega) = h_\xi - \omega j_x$ is diagonalized in $|\xi\alpha\rangle$ to obtain the cranked Nilsson levels and cranked deformed signature basis $|\mu\alpha\rangle$,
2. Construct the Cranked Many-Particle Configuration (CMPC) space
3. $H_{CSM}$ is diagonalized in a CMPC space to get eigenstates of CSM Hamiltonian:

$$|\psi\rangle = \sum_i C_i |i\rangle, \quad C_i \text{ is real},$$

$C_i$ is the corresponding probability amplitude.

# 2.1 Theoretical framework of PNC-CSM

**Nilsson Hamiltonian:**

$$h_\xi = \frac{1}{2}\hbar\omega_0[-\nabla_\rho^2 + \frac{1}{3}\varepsilon_2(2\frac{\partial^2}{\partial\zeta^2} - \frac{\partial^2}{\partial\xi^2} - \frac{\partial^2}{\partial\eta^2})$$

$$+\rho^2 - \frac{2}{3}\varepsilon_2\rho^2 P_2(\cos\theta_t) + 2\varepsilon_4\rho^2 P_4(\cos\theta_t)]$$

$$+2\varepsilon_3\rho^2 P_3(\cos\theta_t) \quad +2\varepsilon_6\rho^2 P_6(\cos\theta_t)$$

$$-2\kappa\hbar\omega_{00}[\vec{l}_t\cdot\vec{s} - \mu(\vec{l}_t^{\,2} - \langle\vec{l}_t^{\,2}\rangle_N)] \quad -\omega j_x$$

S.G. Nilsson, *et al.*,
*Nucl. Phys. A* 1,131 (1969) .

# 2.1 Theoretical framework of PNC-CSM

## Cranked Shell Model (CSM) Hamiltonian:

$$
\begin{aligned}
H_{\mathrm{CSM}} &= H_{\mathrm{SP}} - \omega J_x + H_{\mathrm{P}}(0) + H_{\mathrm{P}}(2) \\
&= \underline{\sum_{\xi} h_{\xi} - \omega J_x} \; \underline{- G_0 \sum_{\xi\eta} a_{\xi}^{\dagger} a_{\bar{\xi}}^{\dagger} a_{\bar{\eta}} a_{\eta} - G_2 \sum_{\xi\eta} q_2(\xi) q_2(\eta) a_{\xi}^{\dagger} a_{\bar{\xi}}^{\dagger} a_{\bar{\eta}} a_{\eta}} \ ,
\end{aligned}
$$

1. $h_0(\omega) = h_\xi - \omega j_x$ is diagonalized in $|\xi\alpha\rangle$ to obtain the cranked Nilsson levels and cranked deformed signature basis $|\mu\alpha\rangle$.
2. Construct the Cranked Many-Particle Configuration (CMPC) space
3. $H_{CSM}$ is diagonalized in a CMPC space to get eigenstates of CSM Hamiltonian:

$$|\psi\rangle = \sum_i C_i |i\rangle, \quad C_i \text{ is real,}$$

$C_i$ is the corresponding probability amplitude.

# 2.1 Theoretical framework of PNC-CSM

## Cranked Shell Model (CSM) Hamiltonian:

$$H_{\mathrm{CSM}} = H_{\mathrm{SP}} - \omega J_x + H_{\mathrm{P}}(0) + H_{\mathrm{P}}(2)$$
$$= \sum_{\xi} h_{\xi} - \omega J_x - G_0 \sum_{\xi\eta} a_{\xi}^{\dagger} a_{\bar{\xi}}^{\dagger} a_{\bar{\eta}} a_{\eta} - G_2 \sum_{\xi\eta} q_2(\xi) q_2(\eta) a_{\xi}^{\dagger} a_{\bar{\xi}}^{\dagger} a_{\bar{\eta}} a_{\eta} \ ,$$

1. $h_0(\omega) = h_{\xi} - \omega j_x$ is diagonalized in $|\xi\alpha\rangle$ to obtain the cranked Nilsson levels and cranked deformed signature basis $|\mu\alpha\rangle$.
2. Construct the Cranked Many-Particle Configuration (CMPC) space
3. $H_{CSM}$ is diagonalized in a CMPC space to get eigenstates of CSM Hamiltonian:

$$|\psi\rangle = \sum_i C_i |i\rangle, \quad C_i \text{ is real},$$

$C_i$ is the corresponding probability amplitude.

# How to construct CMPC space

- A CMPC of a n-particle system reads:

$$|i\rangle = |\mu_1 \mu_2 \cdots \mu_n\rangle = b^\dagger_{\mu_1} b^\dagger_{\mu_2} \cdots b^\dagger_{\mu_n} |0\rangle$$

**The real particles creation operator in cranked deformed basis!**

denotes an occupation of particles in cranked orbitals.

- For each $|i\rangle$ ,

$h_{Nil}(\varepsilon_2, \varepsilon_4, \omega)$

CMPC energy: $E_i = \sum_{\mu_i(occupied)} \varepsilon_{\mu_i}$

Parity: $P_i = \prod_{\mu_i(occupied)} \pi_{\mu_i}$

Signature: $\alpha_i = (\sum_{\mu_i(occupied)} \alpha_{\mu_i}) \bmod 2$

$h_{Nil}(\varepsilon_2, \varepsilon_3, \varepsilon_4, \omega)$

CMPC energy: $E_i = \sum_{\mu_i (\text{occ.})} \varepsilon_{\mu_i}$

Simplex: $s_i = \prod_{\mu_i (\text{occ.})} s_{\mu_i}$

## CMPC truncation :

All possible CMPCs satisfied $E_i - E_0 \le E_C$ construct the CMPC space.

$E_C$ : the truncation (cutoff) energy； $E_0$ : the lowest CMPC energy.

**Diagonalization space will be reduced dramatically!**

# 2.1 Theoretical framework of PNC-CSM

## Cranked Shell Model (CSM) Hamiltonian:

$$H_{\mathrm{CSM}} = H_{\mathrm{SP}} - \omega J_x + H_{\mathrm{P}}(0) + H_{\mathrm{P}}(2)$$
$$= \sum_{\xi} h_{\xi} - \omega J_x - G_0 \sum_{\xi\eta} a^{\dagger}_{\xi} a^{\dagger}_{\bar{\xi}} a_{\bar{\eta}} a_{\eta} - G_2 \sum_{\xi\eta} q_2(\xi) q_2(\eta) a^{\dagger}_{\xi} a^{\dagger}_{\bar{\xi}} a_{\bar{\eta}} a_{\eta} \ ,$$

1. $h_0(\omega) = h_{\xi} - \omega j_x$ is diagonalized in $|\xi\alpha\rangle$ to obtain the cranked Nilsson levels and cranked deformed signature basis $|\mu\alpha\rangle$.
2. Construct the Cranked Many-Particle Configuration (CMPC) space
3. $H_{CSM}$ is diagonalized in a CMPC space to get eigenstates of CSM Hamiltonian:

$$|\psi\rangle = \sum_i C_i |i\rangle, \quad C_i \text{ is real},$$

$C_i$ is the corresponding probability amplitude.

# 2.1 Theoretical framework of PNC-CSM

## Cranked Shell Model (CSM) Hamiltonian:

$$
\begin{aligned}
H_{\mathrm{CSM}} &= H_{\mathrm{SP}} - \omega J_x + H_{\mathrm{P}}(0) + H_{\mathrm{P}}(2) \\
&= \underline{\sum_{\xi} h_{\xi} - \omega J_x} - \underline{G_0 \sum_{\xi\eta} a_{\xi}^{\dagger} a_{\bar{\xi}}^{\dagger} a_{\bar{\eta}} a_{\eta} - G_2 \sum_{\xi\eta} q_2(\xi) q_2(\eta) a_{\xi}^{\dagger} a_{\bar{\xi}}^{\dagger} a_{\bar{\eta}} a_{\eta}} \ ,
\end{aligned}
$$

1. $h_0(\omega) = h_{\xi} - \omega j_x$ is diagonalized in $|\xi\alpha\rangle$ to obtain the cranked Nilsson levels and cranked deformed signature basis $|\mu\alpha\rangle$
2. Construct the Cranked Many-Particle Configuration (CMPC) space
3. $H_{CSM}$ is diagonalized in a CMPC (**truncated Fock**) space to get eigenstates of CSM Hamiltonian:

$$
|\psi\rangle = \sum_i C_i |i\rangle, \quad C_i \text{ is real,}
$$

$C_i$ is the corresponding probability amplitude.

**C. S. Wu, J. Y. Zeng, PRC, 39 (1989) 666**
**J. Y. Zeng, et al., PRC, 50 (1994) 746 &1388**

# 2.1 Theoretical framework of PNC-CSM

**For the seniority ν = 0 ground state ($K^{\pi} = 0^{+}$):**

$$|i\rangle = |\mu_1\bar{\mu}_1 \cdots \mu_k\bar{\mu}_k\rangle = b^{\dagger}_{\mu_1} b^{\dagger}_{\bar{\mu}_1} \cdots b^{\dagger}_{\mu_k} b^{\dagger}_{\bar{\mu}_k} |0\rangle$$

**For the seniority ν = 1 state:**

$$|i\rangle = |\sigma_1\mu_1\bar{\mu}_1 \cdots \mu_k\bar{\mu}_k\rangle = b^{\dagger}_{\sigma_1} b^{\dagger}_{\mu_1} b^{\dagger}_{\bar{\mu}_1} \cdots b^{\dagger}_{\mu_k} b^{\dagger}_{\bar{\mu}_k} |0\rangle, \qquad (\sigma \neq \mu),$$

**For the seniority ν = 2 state:**

$$|i\rangle = |\sigma_1\sigma_2\mu_1\bar{\mu}_1 \cdots \mu_k\bar{\mu}_k\rangle = b^{\dagger}_{\sigma_1} b^{\dagger}_{\sigma_2} b^{\dagger}_{\mu_1} b^{\dagger}_{\bar{\mu}_1} \cdots b^{\dagger}_{\mu_k} b^{\dagger}_{\bar{\mu}_k} |0\rangle, \qquad (\sigma \neq \mu),$$

$(\sigma_1\bar{\sigma}_2)$, $(\bar{\sigma}_1\sigma_2)$ and $(\bar{\sigma}_1\bar{\sigma}_2)$ are considered too, then:

$$K = |\Omega_{\sigma_1} \pm \Omega_{\sigma_2}| \text{ and } \alpha = 0, 1. \qquad \pi = (-)^{N_{\sigma_1} + N_{\sigma_2}}.$$

**For higher seniority ν > 2 state: …… similarly**

- ✓ **The converged solution can always be obtained even for a pair-broken state.**
- ✓ **The Pauli blocking effects is treated spontaneously.**
- ✓ **Provide a reliable way to assign the configuration of a multi-particle state.**

# 2.2 Application of PNC-CSM

## Applications of PNC pairing method

- **Normal deformed nuclei in A = 170 mass region.**
  - J. Y. Zeng, et al., PRC50, 1388 (1994); PRC 65 (2002); PRC 65 (2002).
  - C. S. Wu and J. Y. Zeng, PRC44, 2566 (1991).
  - S. X. Liu and J. Y. Zeng, PRC66, 067301 (2002); NPA 735, 77 (2004).
- **Superdeformed nuclei in A = 150, 190 mass region**
  - C. S. Wu, L. Cheng, C. Z. Lin, and J. Y. Zeng, PRC 45, 2507 (1992).
  - S. X. Liu, J. Y. Zeng, and E. G. Zhao, PRC 66, 024320 (2002); NPA36, 269 (2004)
  - J. Y. Zeng, J. Meng, C. S. Wu, E. G. Zhao, Z. Xing, and X. Q. Chen, PRC44, R1745 (1991).
  - XTH, S. Y. Yu, J. Y. Zeng, and E. G. Zhao, NPA 760, 263 (2005).
- **Superdeformation of light Z ≈ N nuclei in A = 40 mass region**
  - X.-H. Xiang and XTH, CPC 42, 54105 (2018).
  - Yu. Wang and XTH, Description for normal-deformed rotational bands of Cr and Fe isotopes, in preparing.

# 2.2 Application of PNC-CSM

## Applications of PNC pairing method

- **Heaviest actinides and light superheavy nuclei around Z = 100 mass region**
  - XTH and Shu-yong Zhao, Chin. Phys. C 44, 034106 (2020).
  - Y.-C. Li and XTH, SCP Mech & Astro 59 (2016).
  - Z.-H Zhang et al., SCP Mech&Astro 59, 672012 (2016), PRC 87, 1 (2013). PRC 83,1 (2011)
  - Z.-H. Zhang, XTH, J.-Y. Zeng, E.-G. Zhao, and S.-G. Zhou, PRC 85, 1 (2012).
  - XTH, Z.-Z. Ren, S.-X. Liu, and E.-G. Zhao, NPA 817, 45 (2009).
- **High-K isomers in the rare-earth and actinide nuclei mass region**
  - XTH, Yang Cao and Xiao-Ling Gan, Phys. Rev. C 102, 014322 (2020).
  - Shuo-Yi Liu, Miao Huang, and Zhen-Hua Zhang, Phys. Rev. C **100**, 064307 (2019).
  - XTH and Y. C. Li, Phys. Rev. C **98**, 064314 (2018).
  - Zhen-Hua Zhang, Phys. Rev. C **98**, 034304 (2018)
  - B.-H. Li, Z.-H. Zhang, and Y.-A. Lei, CPC 37, 014101 (2013).
  - Z. H. Zhang, Y. A. Lei, and J. Y. Zeng, PRC 80, 034313 (2009); NPA 816, 19 (2009).

# 2.2 Application of PNC-CSM

PNC pairing method has been implemented to other nuclear theoretical models successfully:

- **to the covariant density functional theory→ Shell-model-like approach (SLAP)**
  - Zhen-Hua Zhang, Miao Huang, and A. V. Afanasjev, Phys. Rev. C **101**, 054303 (2020).
  - **Lang Liu, Phys. Rev. C 99, 024317 (2019).**
  - Z. Shi, Z. H. Zhang, Q. B. Chen, S. Q. Zhang, and J. Meng, PRC 97, 034317 (2018).

- **to the total-routhian-surface (TRS) model**
  - X. M. Fu, F.R.Xu, J.C.Pei, et al., PRC 87(2013); PRC 89, 1 (2014).
  - W. Y. Liang, C. F. Jiao, Q. Wu, X. M. Fu, and F. R. Xu, PRC 92, 064325 (2015).

# 3. Results and discussions

# 3.1 High-*j* intruder proton orbitals

We include **the proton $N = 7$ shell** to construct the CMPC space and find that the **1 *j*15/2(1/2 [770])** orbital plays an important role in the rotational properties of $^{251}$Md

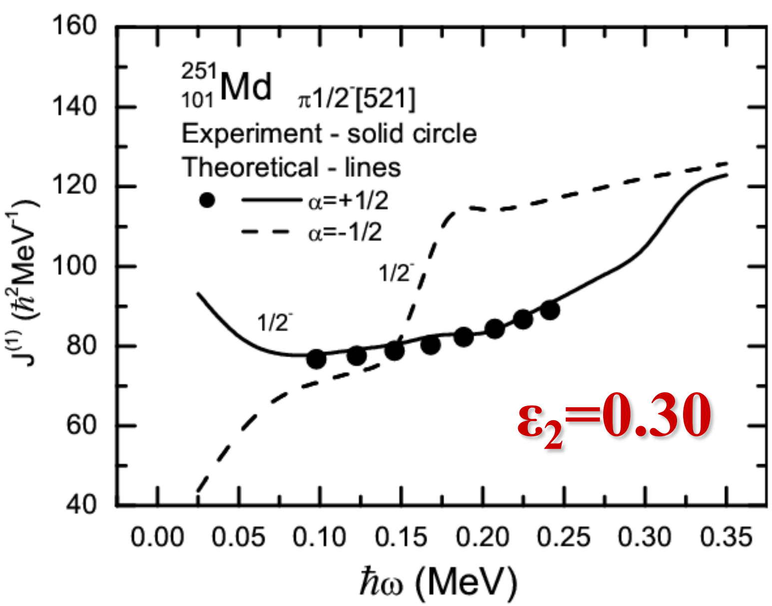


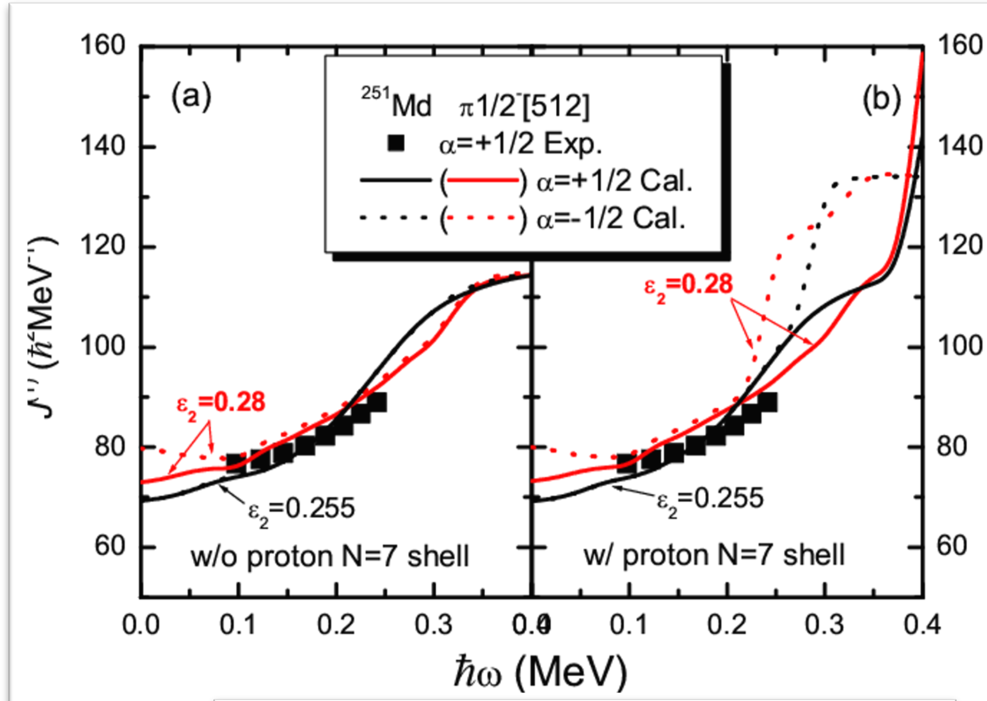


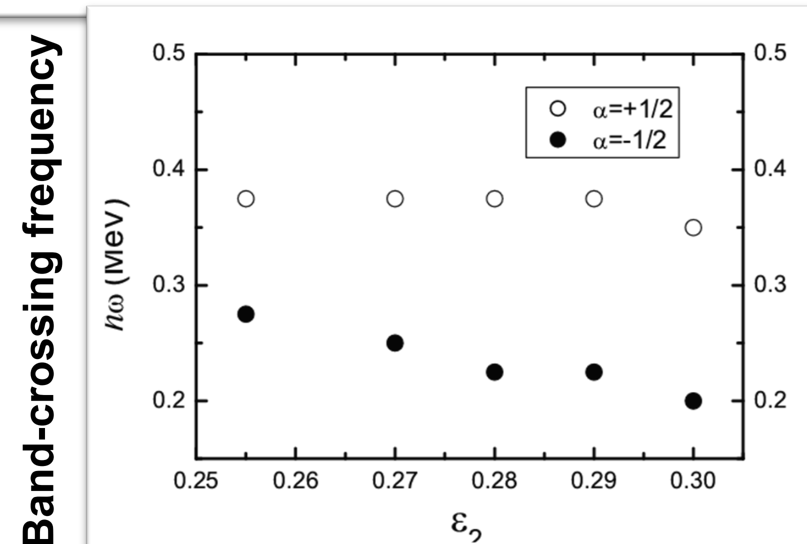


XTH, Z. Z Ren, S. X. Liu, E. G Zhao, Nucl. Phys. A 817, 45 (2009).

# 3.1 High-*j* intruder proton orbitals

**The bandhead spins are assigned:**
196.6(5) keV transition : $13/2^- \rightarrow 9/2^-$
189(1) keV transition : $11/2^- \rightarrow 7/2^-$

**We include the proton $N = 7$ shell to construct the CMPC space and find that the 1 $j$15/2(1/2 [770]) orbital plays an important role in the rotational properties of $^{255}$Lr**

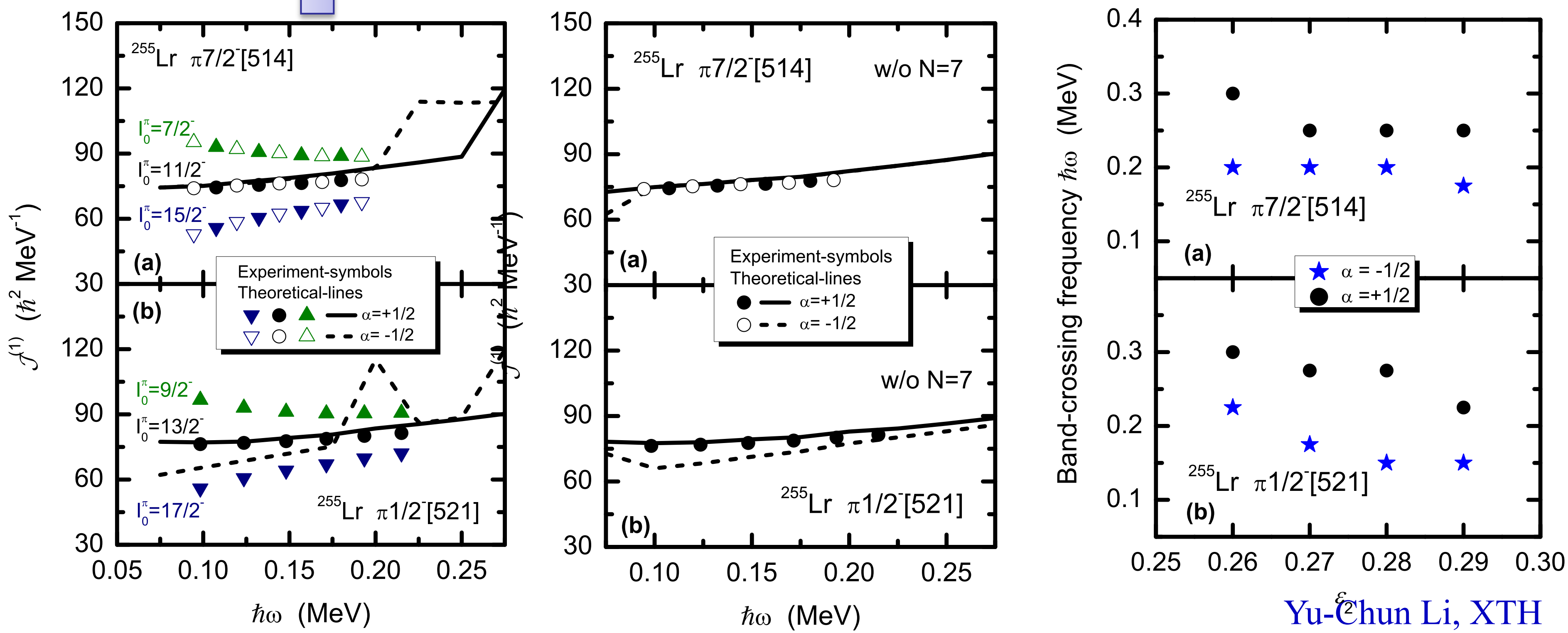


Yu-Chun Li, XTH
Sci. China-Phys. Mech. Astron. **59**, 672011 (2016).

# 3.2 Systematic study of the GSB

**Nilsson parameters ($\kappa$, $\mu$)** : By fitting the experimental single-particle levels in the odd-$A$ nuclei with **Z=96-103 (A=240-255)** (more than **30** nuclei), a new set of Nilsson parameters ($\kappa$, $\mu$) are obtained, which are dependent on the main oscillator quantum number $N$ as well as the orbital angular momentum $l$.

| $N$ | $l$ | $\kappa_p$ | $\mu_p$ | $N$ | $l$ | $\kappa_n$ | $\mu_n$ |
|---|---|---|---|---|---|---|---|
| 4 | 0,2,4 | 0.0670 | 0.654 | | | | |
| 5 | 1 | 0.0250 | 0.710 | 6 | 0 | 0.1600 | 0.320 |
| | 3 | 0.0570 | 0.800 | | 2 | 0.0640 | 0.200 |
| | 5 | 0.0570 | 0.710 | | 4,6 | 0.0680 | 0.260 |
| 6 | 0,2,4,6 | 0.0570 | 0.654 | 7 | 1,3,5,7 | 0.0634 | 0.318 |

Z. H. Zhang, XTH, J. Y. Zeng, E. G. Zhao and S. G. Zhou, *Phys. Rev. C* 85, 014324 (2012).
Z.-H. Zhang, J.-Y. Zeng, E.-G. Zhao, and S.-G. Zhou, *Phys. Rev. C* 83, 011304(R) (2011).

# 3.2 Systematic study of the GSB

**Nilsson parameters ($\kappa$, $\mu$) :** By fitting the experimental single-particle levels in the odd-*A* nuclei with **Z=96-103 (A=240-255)** (more than **30** nuclei), a new set of Nilsson parameters ($\kappa$, $\mu$) are obtained, which are dependent on the main oscillator

**The root-mean-square** deviation of theoretical 1-qp band-head energies from the experimental values for **Z=96-103(A=240-255)** nuclei is about 270 keV (200 keV by using the Woods-Saxon potential) for neutrons by this new set of ($\kappa$, $\mu$).

| | | | | | | | |
|---|---|---|---|---|---|---|---|
| | 3 | 0.0570 | 0.800 | | 2 | 0.0640 | 0.200 |
| | 5 | 0.0570 | 0.710 | | 4,6 | 0.0680 | 0.260 |
| 6 | 0,2,4,6 | 0.0570 | 0.654 | 7 | 1,3,5,7 | 0.0634 | 0.318 |

Z. H. Zhang, XTH, J. Y. Zeng, E. G. Zhao and S. G. Zhou, *Phys. Rev. C* 85, 014324 (2012).
Z.-H. Zhang, J.-Y. Zeng, E.-G. Zhao, and S.-G. Zhou, *Phys. Rev. C* 83, 011304(R) (2011).

# 3.3 High-order deformation $\varepsilon_6$

Macroscopic-microscopic approach: The inclusion of $\beta_6$ deformation can give extra binding energy in excess of 1 MeV.

**I. Muntian et al., Phys. Lett. B 500, 241 (2001).**

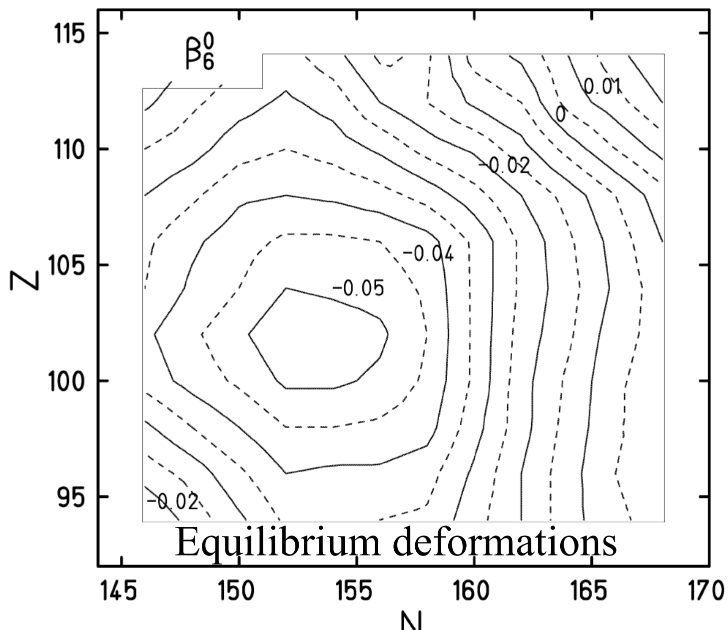

Equilibrium deformations

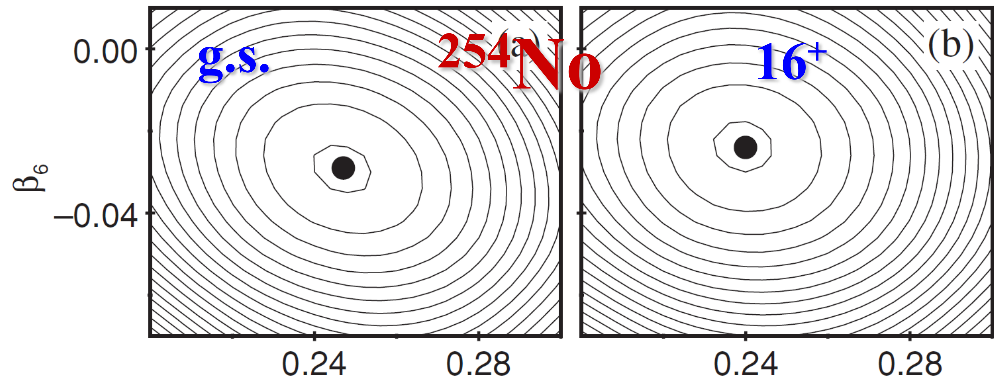


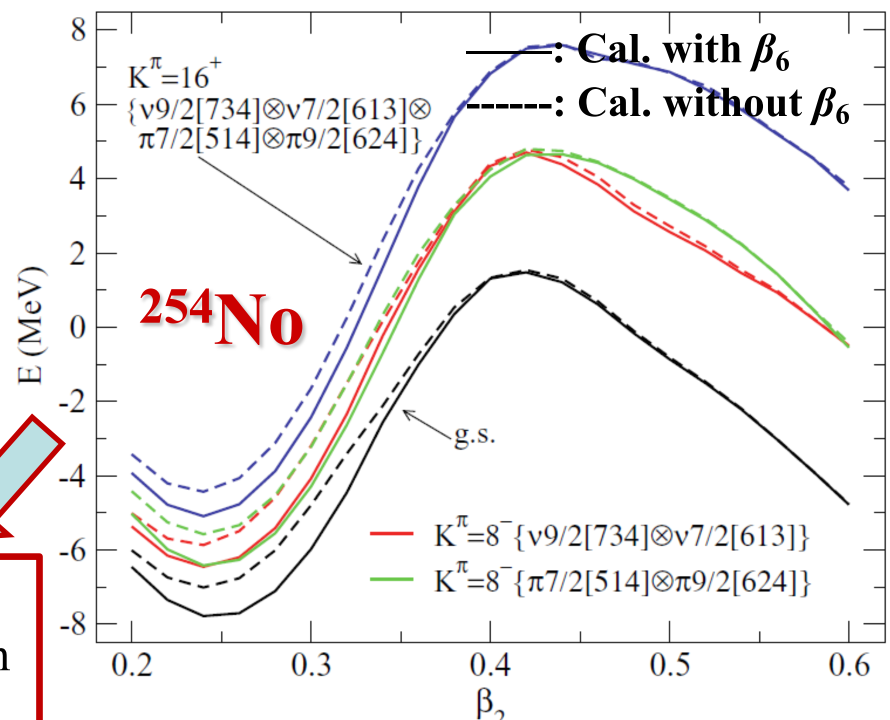


Configuration-constrained potential-energy-surface (PES) calculations→ The isomers gain extra binding energy from the $\beta_6$ deformation, implying enhanced stability against fission.

**H.L. Liu et al., Eur. Phys. J. A. 47, 135 (2011).**
**H.L. Liu et al., Phys. Rev. C 83, 011303(R) (2011).**

# 3.3 High-order deformation $\varepsilon_6$

$\beta_6$ deformation leads to an enlarged $Z = 100$ and $N = 152$ deformed shell gap.

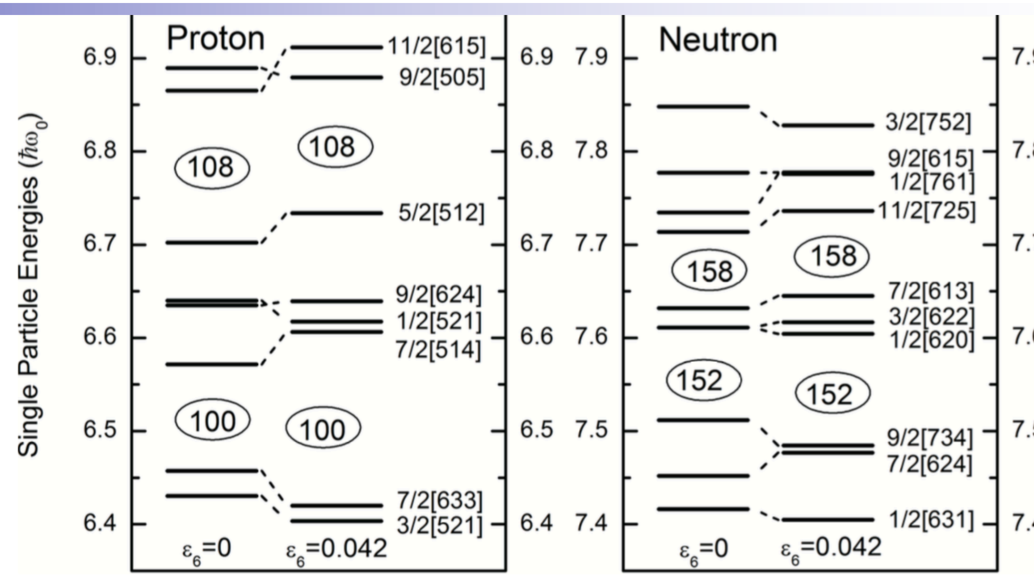


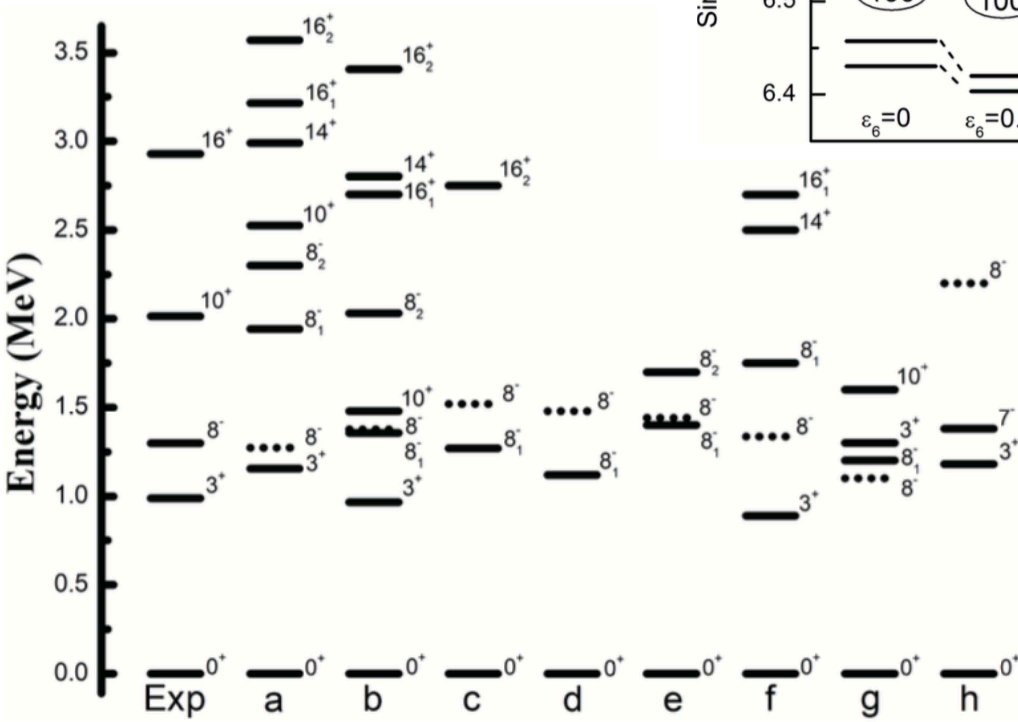


XTH, S. Y. Zhao, Z. H. Zhang and Z. Z. Ren CPC44, 034106 (2020).

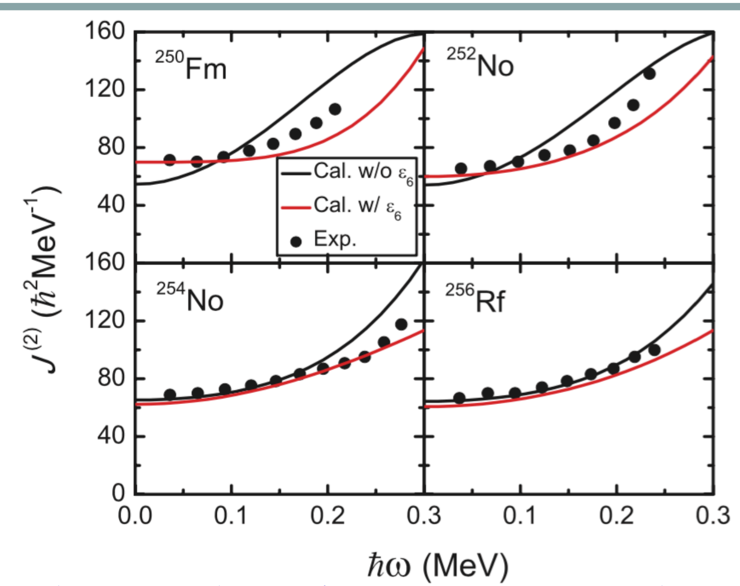


Zhen-Hua Zhang, Jie Meng, En-Guang Zhao and Shan-Gui Zhou, PRC **87**, 054308 (2013)

# 3.3 High-order deformation $\varepsilon_6$

***Reverse of the single-proton levels in Lr isotopes***

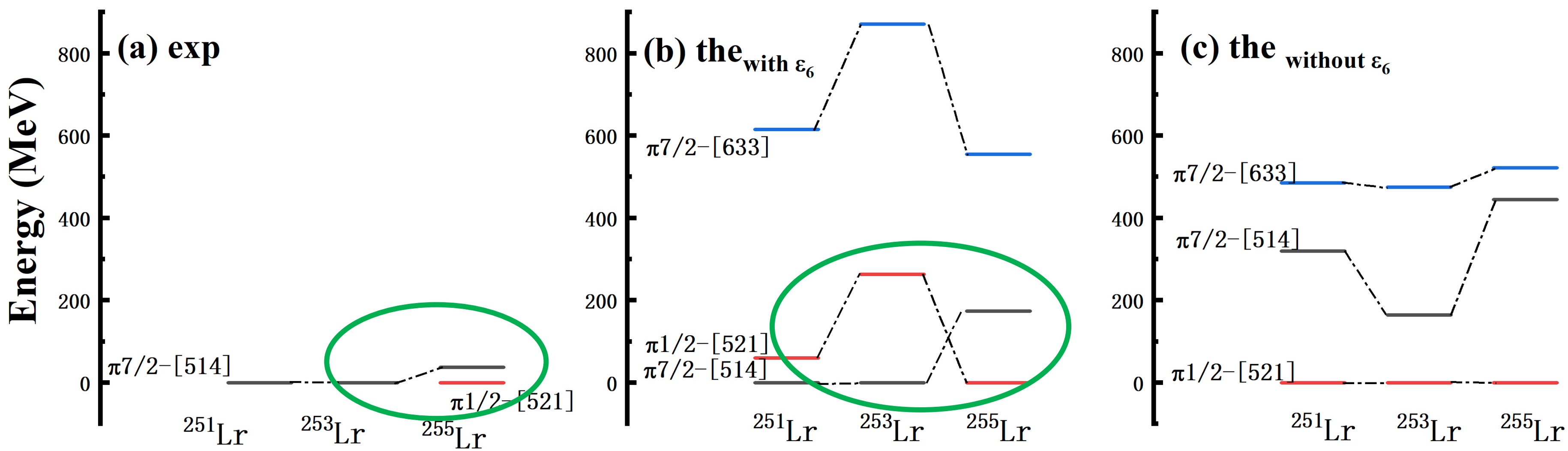


XTH et al., in preparation

T Huang, D. Seweryniak,…, **XTH** et al.,
Phys. Rev. C, 106, L061301 (2022).

# 3.3 High-order deformation $\varepsilon_6$

## *Reverse of the single-proton levels in Lr isotopes*

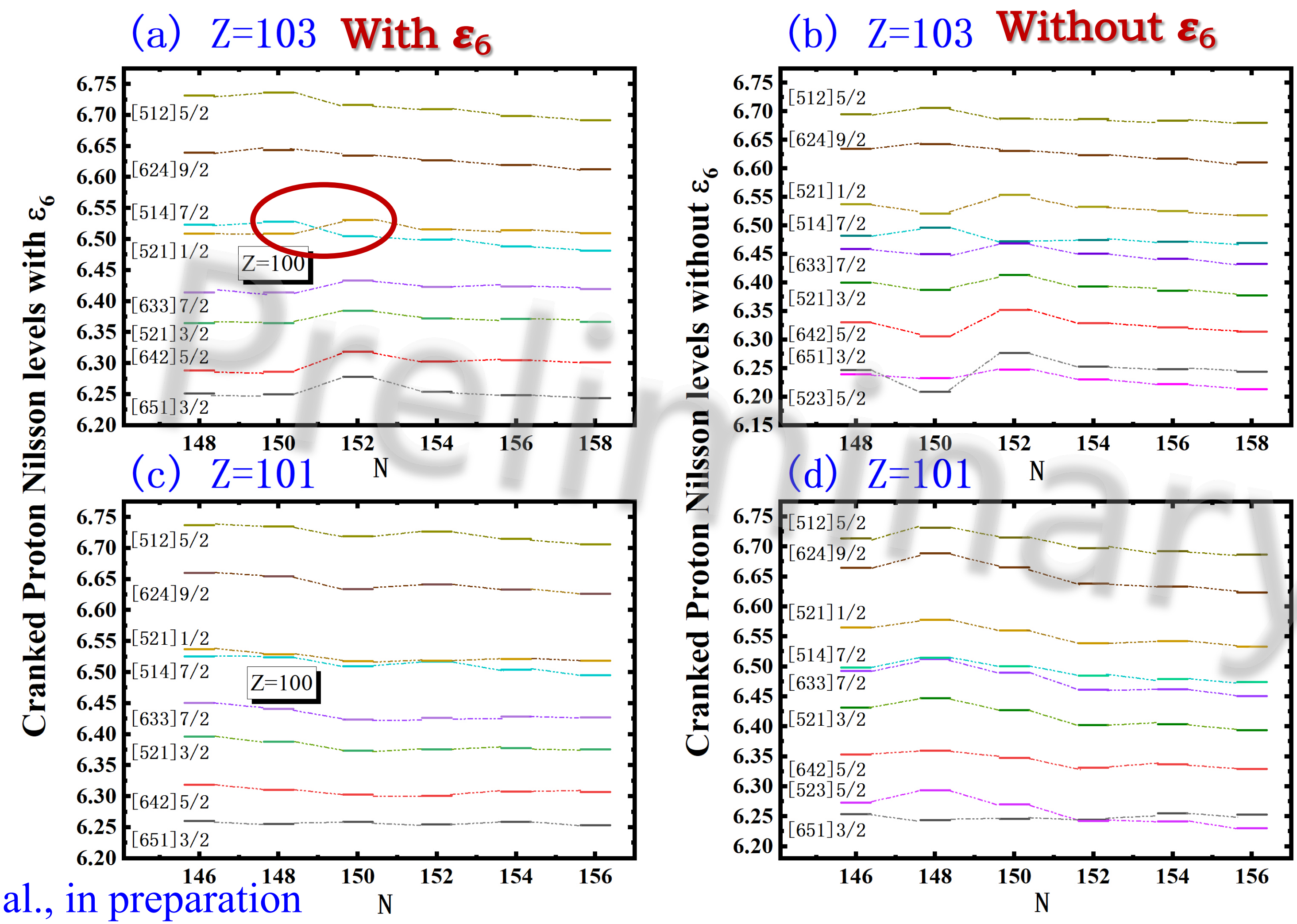


XTH et al., in preparation

# 3.3 High-K isomers

**Nilsson parameters ($\kappa$, $\mu$) :** By fitting the low-lying high-K multi-particle state energy and rotational band in the transfermium nuclei with $100 \leqslant Z \leqslant 105$. A improved new set of Nilsson parameters ($\kappa$, $\mu$) are obtained, where $\boldsymbol{\varepsilon_2}$ $\boldsymbol{\varepsilon_4}$ $\boldsymbol{\varepsilon_6}$ are considered.

**The root-mean-square** deviation of theoretical 1-qp and multi-qp band-head energies from the experimental values for **Z=100-105(A=246-261)** nuclei is about 370 keV by this new set of ($\kappa$, $\mu$).



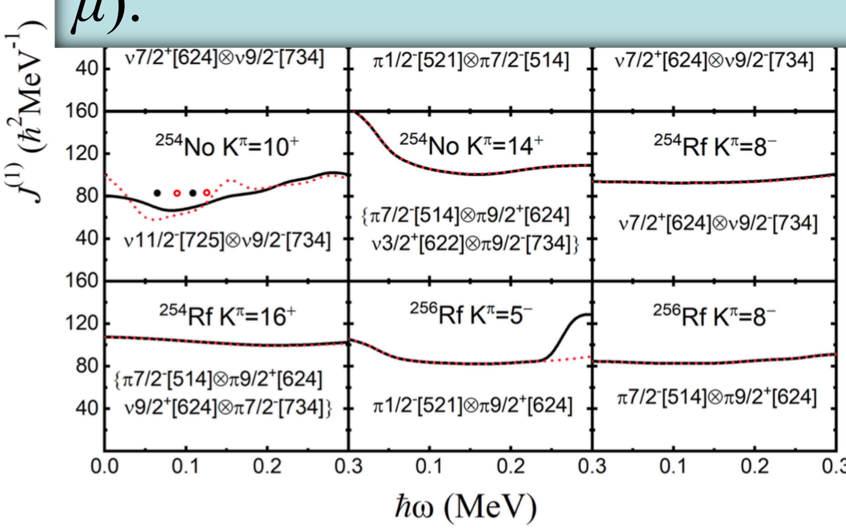


| | | | |
|---|---|---|---|
| $5/2^+$ | $\nu5/2^+[622]$ | 0.8054 | 0.20009 [55] |
| $1/2^+$ | $\nu1/2^+[631]$ | 0.8198 | 0.392 [55] |
| $7/2^+$ | $\nu7/2^+[613]$ | 0.8754 | |
| $^{253}$Fm | | | |
| $1/2^+$ | $\nu1/2^+[620]$ | 0 | 0 [57] |
| $3/2^+$ | $\nu3/2^+[622]$ | 0.1037 | 0.1241 [57] |
| $7/2^+$ | $\nu7/2^+[613]$ | 0.2474 | 0.15 [50] |
| $9/2^-$ | $\nu9/2^-[734]$ | 0.5275 | |
| $7/2^+$ | $\nu7/2^+[624]$ | 0.646 | |
| $11/2^-$ | $\nu11/2^-[725]$ | 0.9174 | 0.361 [50] |
| $9/2^+$ | $\nu9/2^+[615]$ | 1.2207 | 0.548 [50] |
| $^{247}$Md | | | |
| $7/2^-$ | $\pi7/2^-[514]$ | 0 | 0 [58] |
| $1/2^-$ | $\pi1/2^-[521]$ | 0.1959 | 0.153 [58] |
| $7/2^+$ | $\pi7/2^+[633]$ | 0.2686 | |
| $3/2^-$ | $\pi3/2^-[521]$ | 0.6873 | |
| $9/2^+$ | $\pi9/2^+[624]$ | 0.9802 | |
| $^{249}$Md | | | |



**XTH & Jun Zhang, in preparation**

# 3.4 High-K isomers

## $K^{\pi} = 8^{-}$ isomers in N = 150 shell-stabilized isotones

$8^{-}$ $\upsilon^{2}$ {[734]9/2⊗[624]7/2}

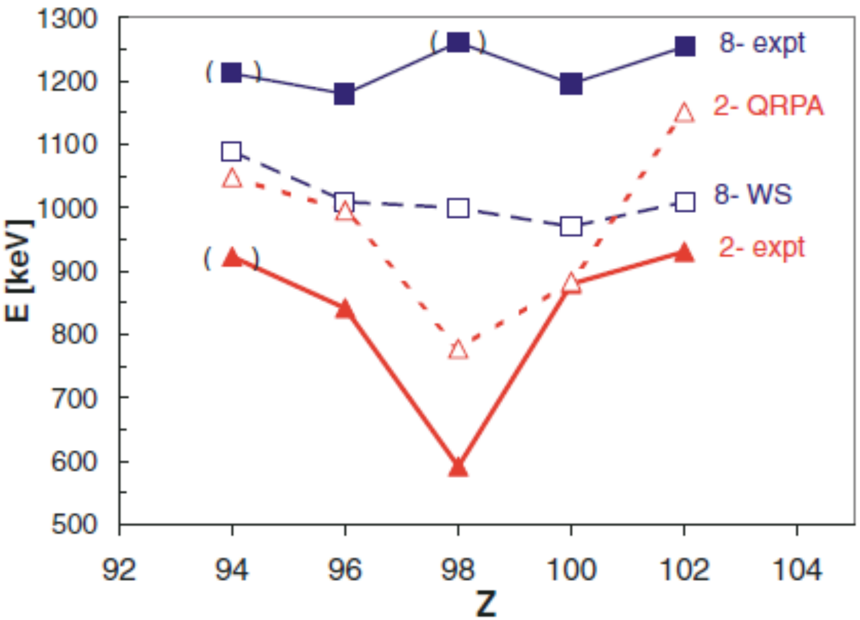


A. P. Robinson et al., Phys. Rev. C **78, 034308 (2008)**

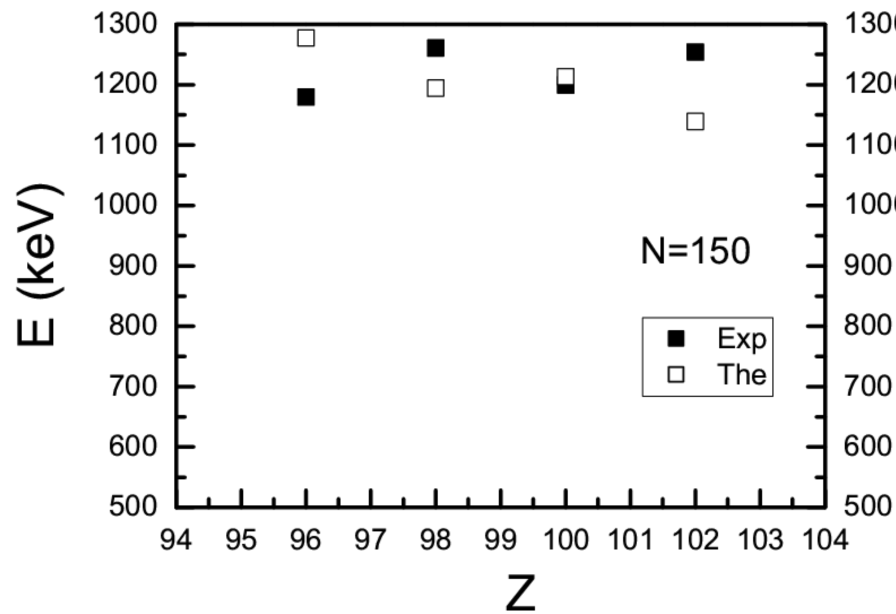


**PNC-CSM calculations**

# 3.4 High-K isomers

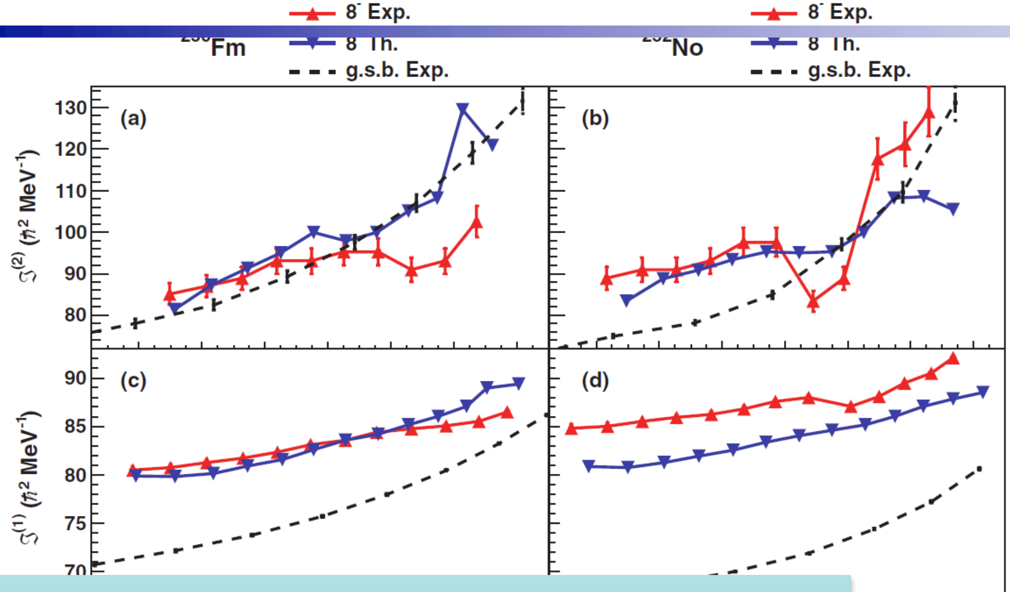


HFB calculation from
B. Sulignano et al.,PRC 86, 044318 (2012)

CCTRS calculationfrom F. R.Xu et al.

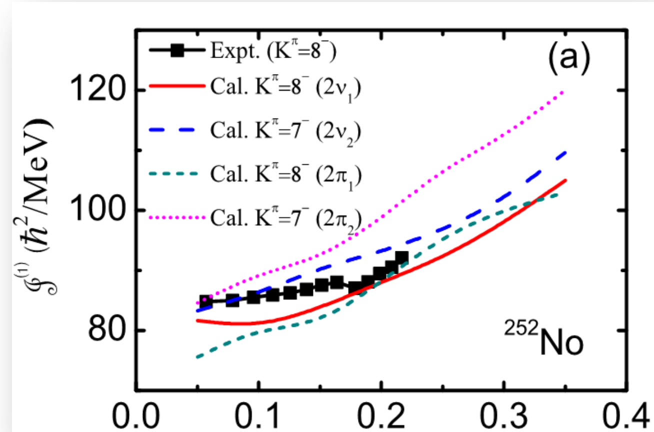


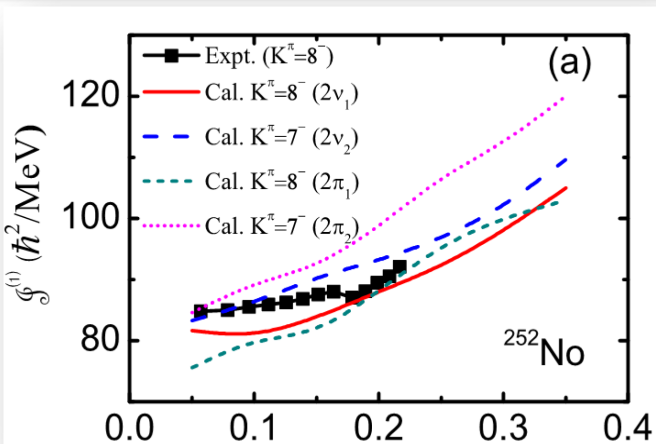


CCTRS calculationfrom F. R.Xu et al.

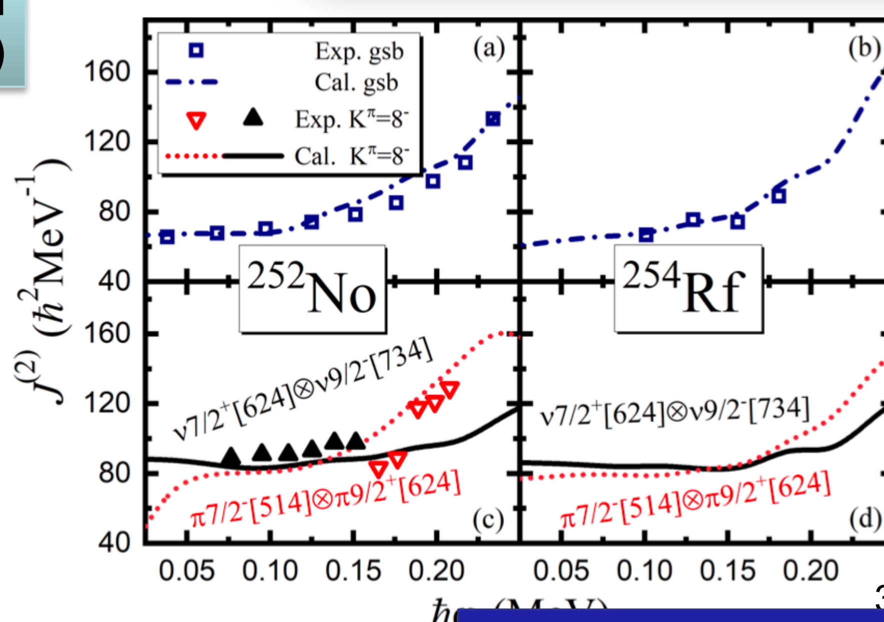


PNC-CSM calculations

# 3.4 High-K isomers-Pairing

## Moments of inertia of the multi-quasiparticle bands in $^{254}$No

A 20% ~ 25% increase in $J^{(1)}$ can be seen for the high−K bands at low frequency.

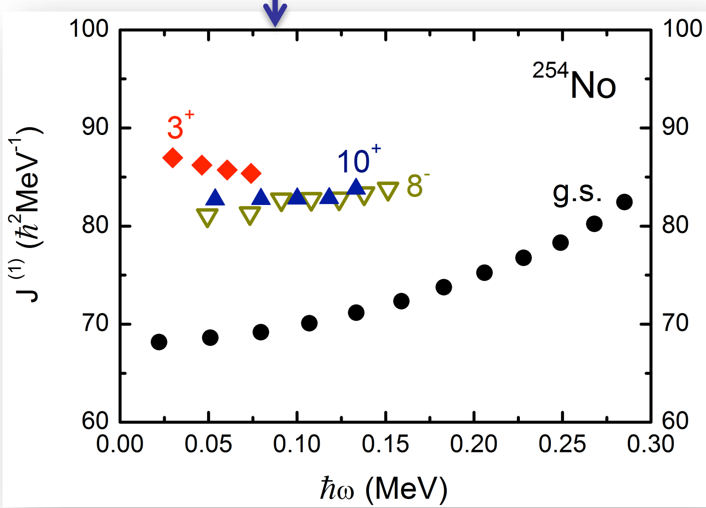


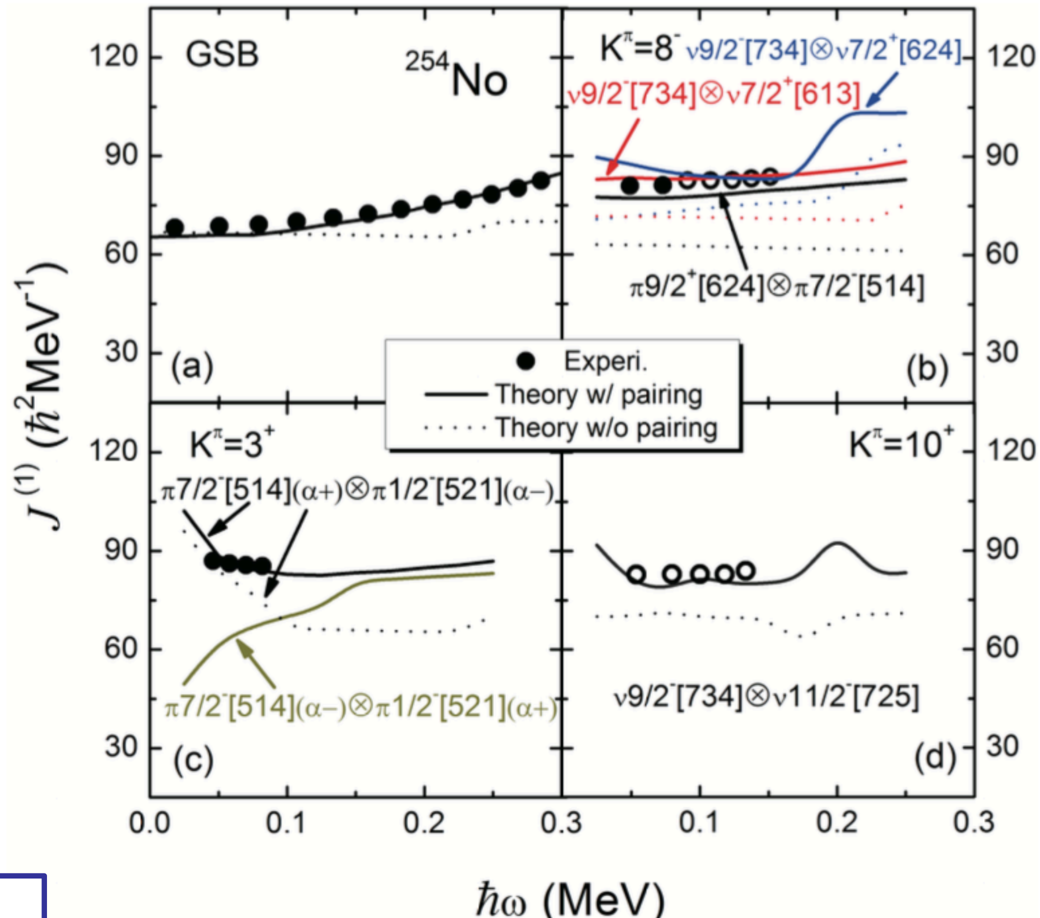


? Configuration of Kp=8-:2p or 2n

XTH, Shu-Yong Zhao, Zhen-hua Zhang, Zhng-Zhou Ren Chin. Phys. C 44 (2020) 034106.

# 3.4 High-K isomers-Pairing

## Pairing reduction of the multi-quasiparticle bands in $^{254}$No

The nuclear pairing gap in the PNC-CSM,

$$\tilde{\Delta} = G_0 \left[ -\frac{1}{G_0} \langle\psi| H_{\mathrm{P}} |\psi\rangle \right]^{1/2} .$$

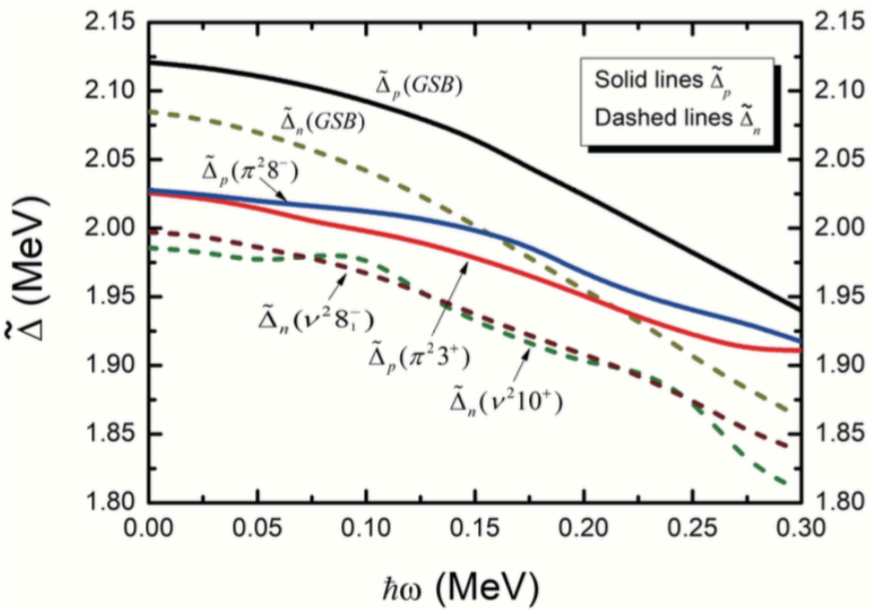


The relative pairing gap reduction factor is defined as,

$$R_\tau(\omega) = \frac{\tilde{\Delta}_\tau(\omega) - \tilde{\Delta}_\tau(\omega=0)}{\tilde{\Delta}_\tau(\omega=0)},$$

$$R_\tau(\nu) = \frac{\tilde{\Delta}_\tau(\nu) - \tilde{\Delta}_\tau(\nu=0)}{\tilde{\Delta}_\tau(\nu=0)}, \qquad \tau = p \text{ or } n$$

| | |
|---|---|
| GSB $:R_p(\omega = 0.3\mathrm{MeV}/\hbar) \approx 18.1\%,$ | |
| $\pi^2 3^+$ $:R_p(\omega = 0.3\mathrm{MeV}/\hbar) \approx 5.7\%,$ | $R_p(\nu = 2) \approx 4.5\%$ |
| $\pi^2 8^-$ $:R_p(\omega = 0.3\mathrm{MeV}/\hbar) \approx 5.4\%,$ | $R_p(\nu = 2) \approx 4.4\%$ |
| GSB $:R_n(\omega = 0.3\mathrm{MeV}/\hbar) \approx 22.3\%,$ | |
| $\nu^2 8_1^-$ $:R_n(\omega = 0.3\mathrm{MeV}/\hbar) \approx 8.0\%,$ | $R_n(\nu = 2) \approx 4.2\%$ |
| $\nu^2 10^+$ $:R_n(\omega = 0.3\mathrm{MeV}/\hbar) \approx 8.0\%,$ | $R_n(\nu = 2) \approx 4.8\%.$ |

The effective pairing interaction strengths: $G_{0p}$=0.25, $G_{2p}$=0.02,
$G_{0n}$=0.25, $G_{2n}$=0.02



XTH, Shu-Yong Zhao, Zhen-hua Zhang, Zhng-Zhou Ren Chin. Phys. C 44 (2020) 034106.

# 3.5 Identical band in $^{255}$Lr and $^{251}$Md

## *Identical band in Lr and Md*

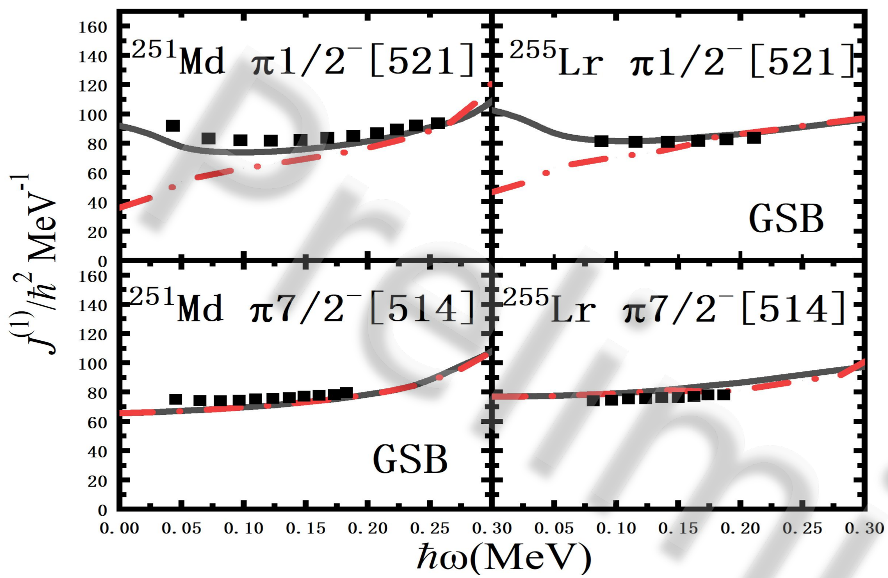


XTH et al., in preparation

R. Briselet,et al.,
Phys. Rev. C 102, 014307 (Jul 2020).

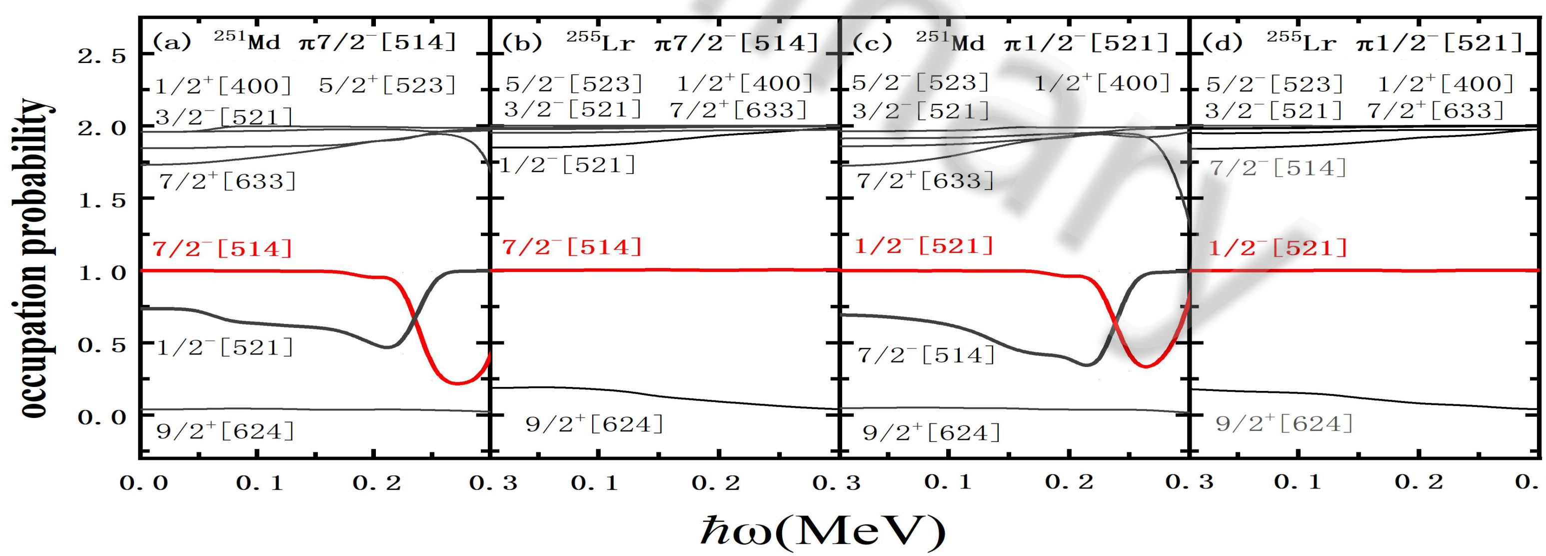

# 3.5 Identical band in Lr and Md isotopes

## *Identical band in Lr and Md*

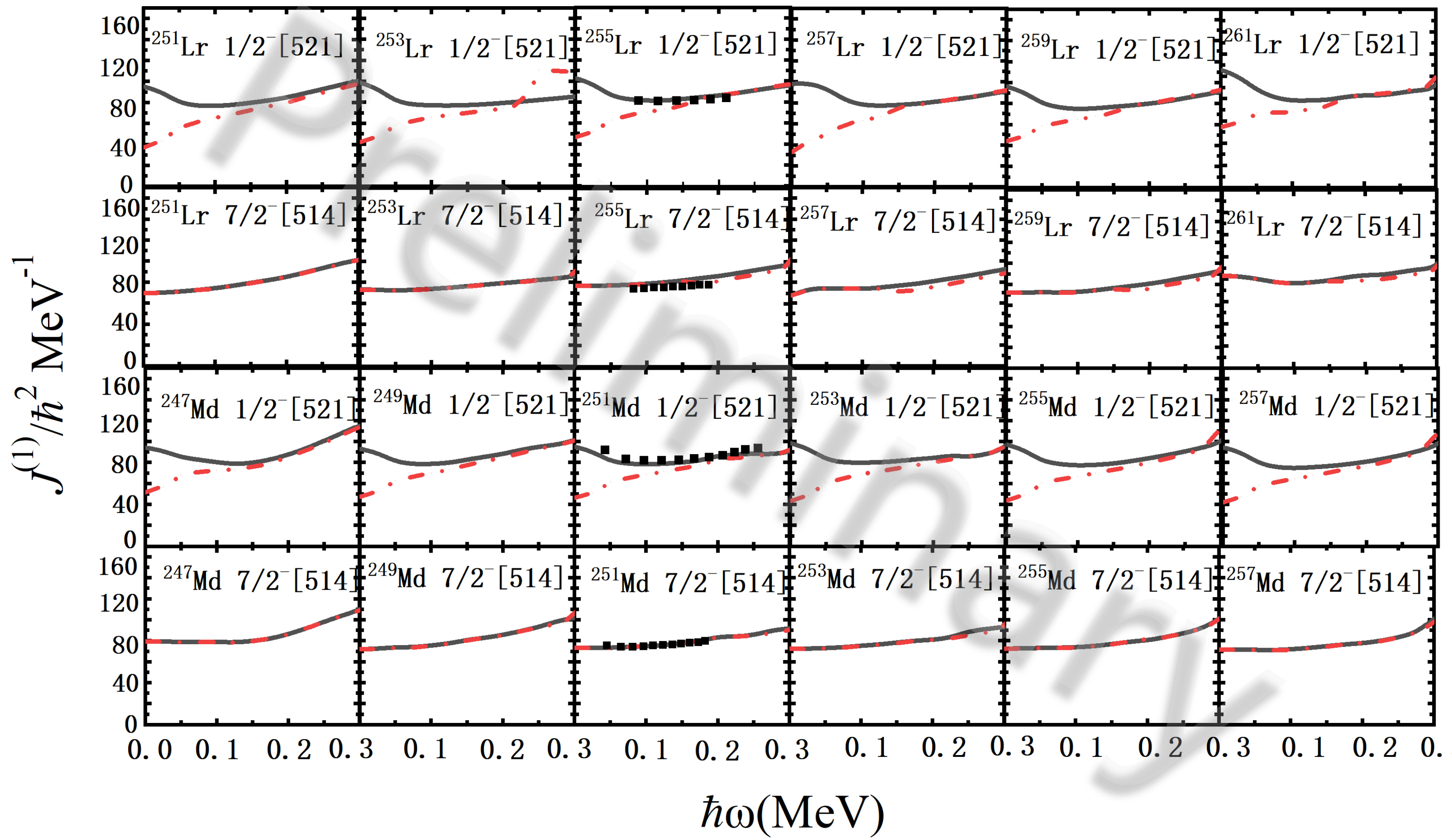




**XTH et al., in preparation**

# 3.6 Octupole deformation $\varepsilon_3$

$$R = \omega(-)/\omega(+).$$

**The limit of static octupole deformation:**

$$\boxed{R \to R_{\text{rigid}} = 1,}$$

**The limit of aligned octupole phonon :**

$$\boxed{R \to (4(I-3)-2)/(4I-2)}$$

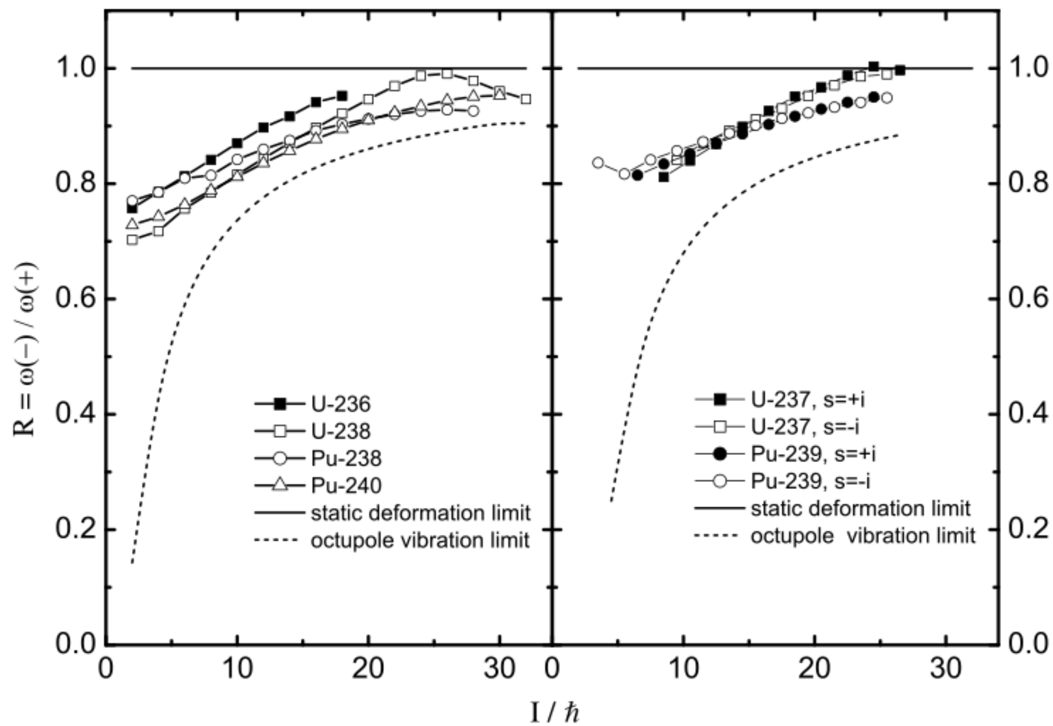


FIG. 1. $R = \omega(-)/\omega(+)$ versus $I$ for even-even nuclei $^{236,238}$U and $^{238,240}$Pu (left) and odd-A nuclei $^{237}$U and $^{239}$Pu (right). The solid (dash) line shows the static octupole deformation limit (octupole vibration limit).

XTH and Yu-Chun Li, Physical Review C 102 (2020)_064328

# 3.6 Octupole deformation $\varepsilon_3$

$$h_{\mathrm{Nil}} = \frac{1}{2}\hbar\omega_0[-\nabla_\rho^2 + \frac{1}{3}\varepsilon_2(2\frac{\partial^2}{\partial\zeta^2} - \frac{\partial^2}{\partial\xi^2} - \frac{\partial^2}{\partial\eta^2}) + \rho^2 - \frac{2}{3}\varepsilon_2\rho^2 P_2(\cos\theta_t) + 2\varepsilon_4\rho^2 P_4(\cos\theta_t)] + 2\varepsilon_3\rho^2 P_3(\cos\theta_t) - 2\kappa\hbar\omega_{00}[\vec{l}_t\cdot\vec{s} - \mu(\vec{l}_t^{\,2} - \langle\vec{l}_t^{\,2}\rangle_N)]$$

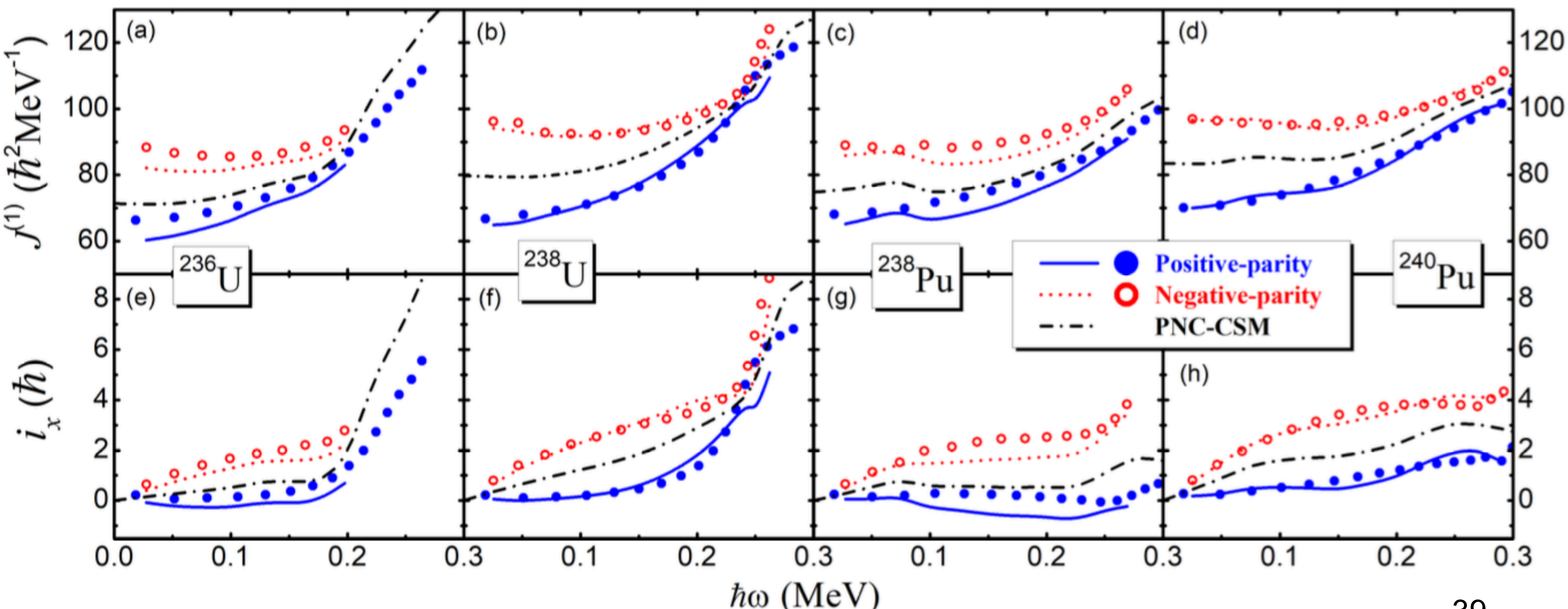




XTH and Yu-Chun Li, Physcial Review C 102 (2020)_064328

# 3.6 Octupole deformation $\varepsilon_3$

The off-diagonal contributions of each sinlge particle levels $j_x(\mu\nu)$ to the angular momentum alignment.

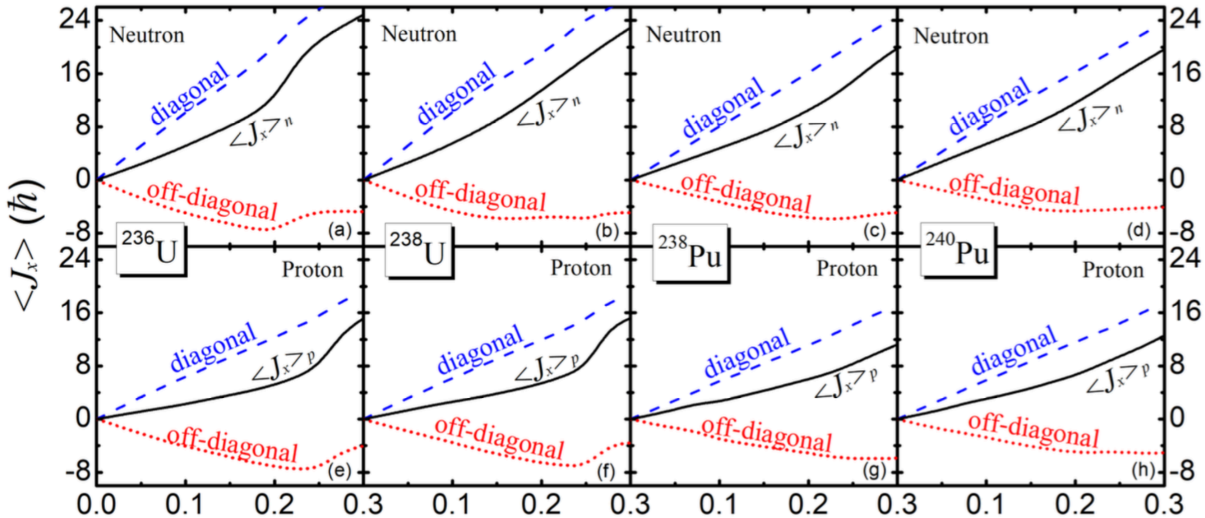


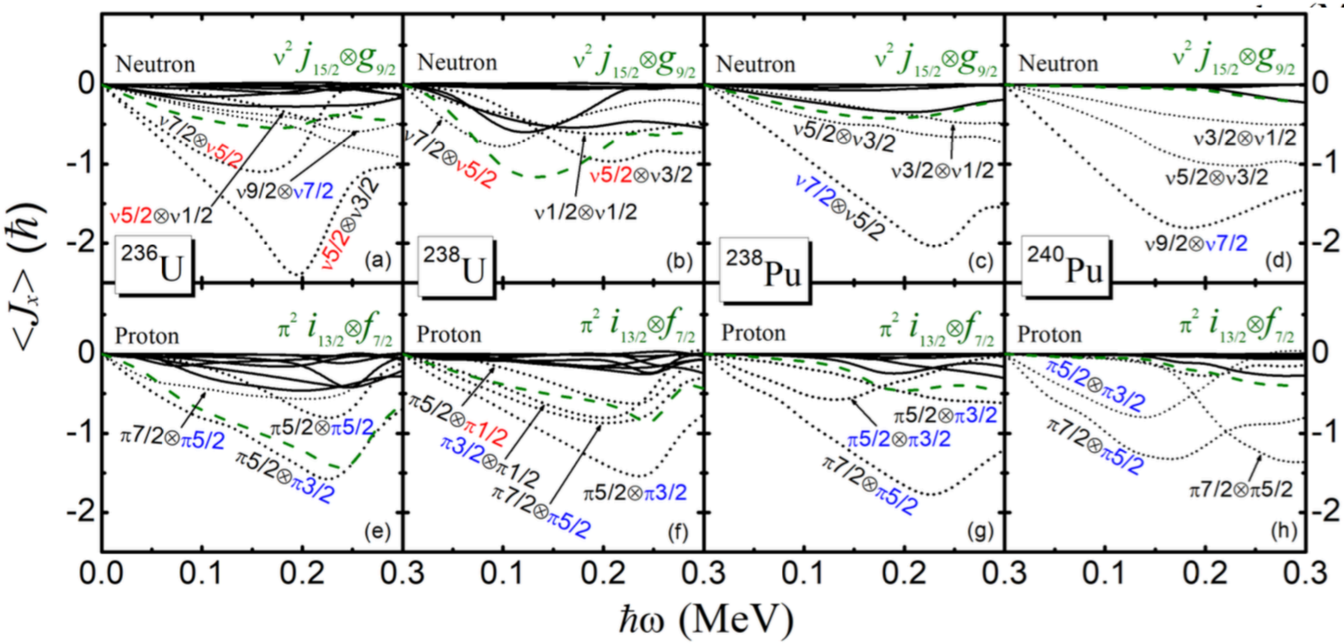


The alignment for nucleons occupying the octupole-deformed pairs of neutron ν2j15/2g9/2 and of proton π2i13/2f7/2 orbitals give a very important contribution to the upbendings.



XTH and Yu-Chun Li, PRC 102 (2020)_064328

# 3.6 Octupole deformation $\varepsilon_3$

## Parity doublet bands in odd-A nuclei:

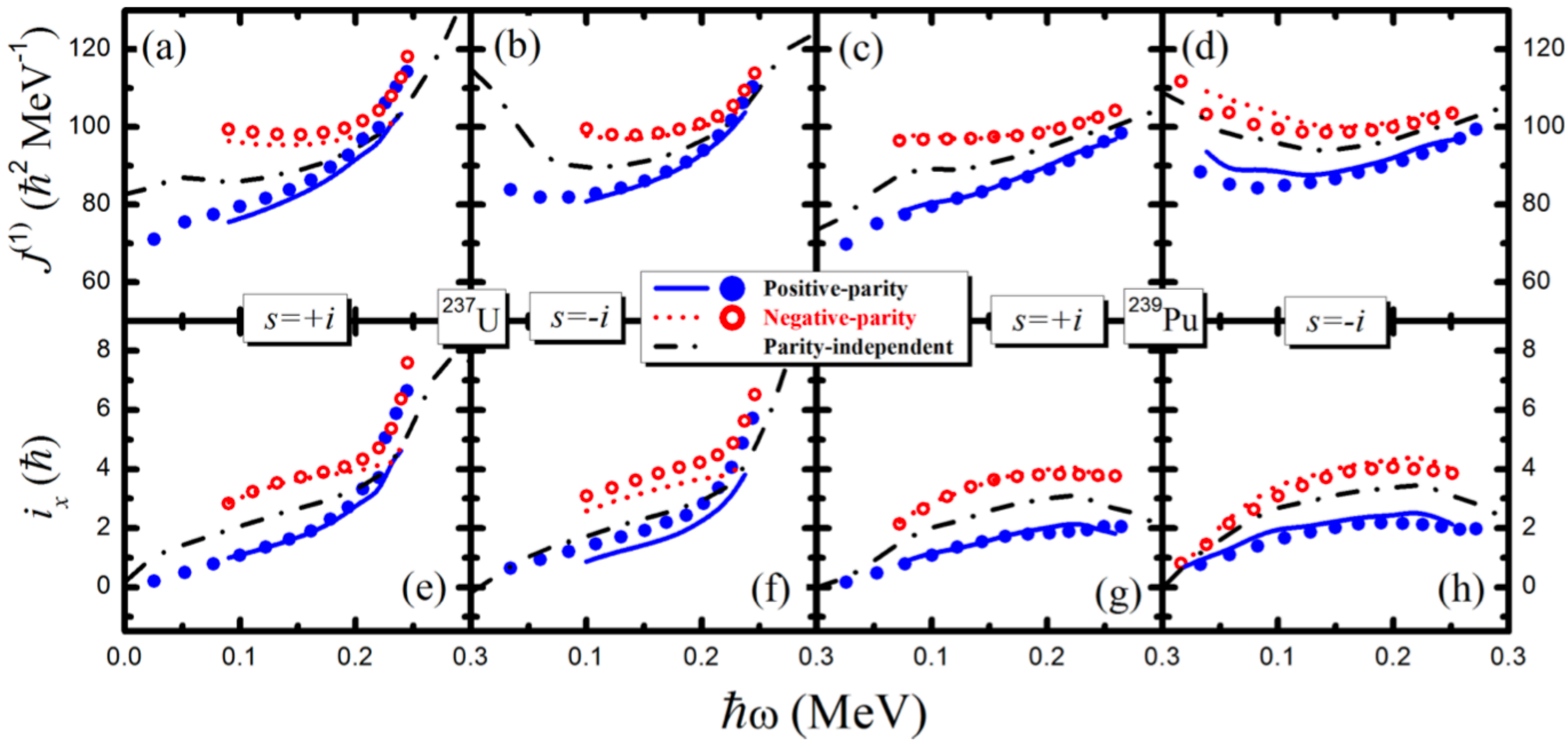


- $^{237}$U 在0.25MeV处有明显上弯，$^{239}$Pu转动带比较平缓;
- $^{237}$U和$^{239}$Pu的s=+i和s=-i转动带之间都存在明显的劈裂(simplex splittings).

Jun Zhang, XTH*, Yu-Chun Li and Hai-Qian Zhang, PRC, 107, 024305 (2023).

# 3.6 Octupole deformation $\varepsilon_3$

## Parity doublet bands in odd-A nuclei:

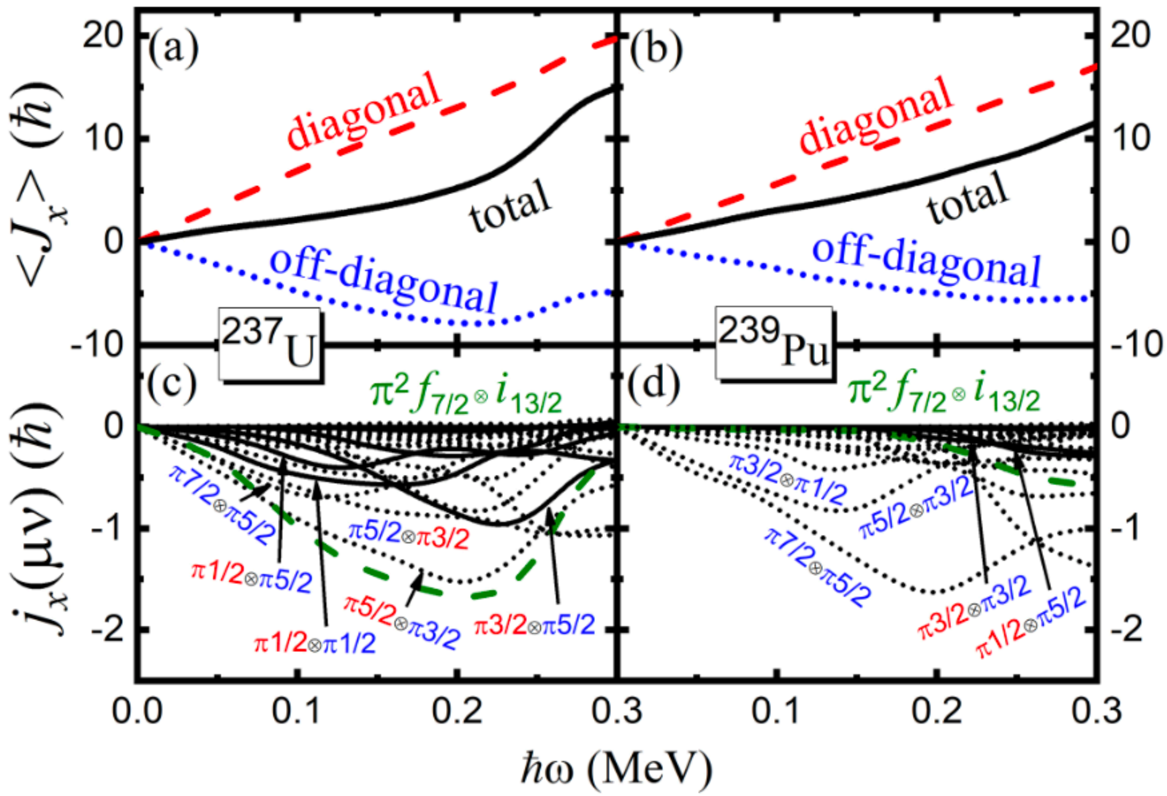


- $^{237}$U顺排的非对角部分导致上弯，且八极关联 $\pi^2 i_{13/2}\otimes f_{7/2}$ 较强，对上弯有明显贡献；
- $^{239}$Pu顺排的对角和非对角部分都比较平缓，八极关联 $\pi^2 i_{13/2}\otimes f_{7/2}$ 贡献小。

Jun Zhang, XTH*, Yu-Chun Li and Hai-Qian Zhang, PRC, 107, 024305 (2023).

# 3.6 Octupole deformation $\varepsilon_3$

## Parity doublet bands in odd-A nuclei:

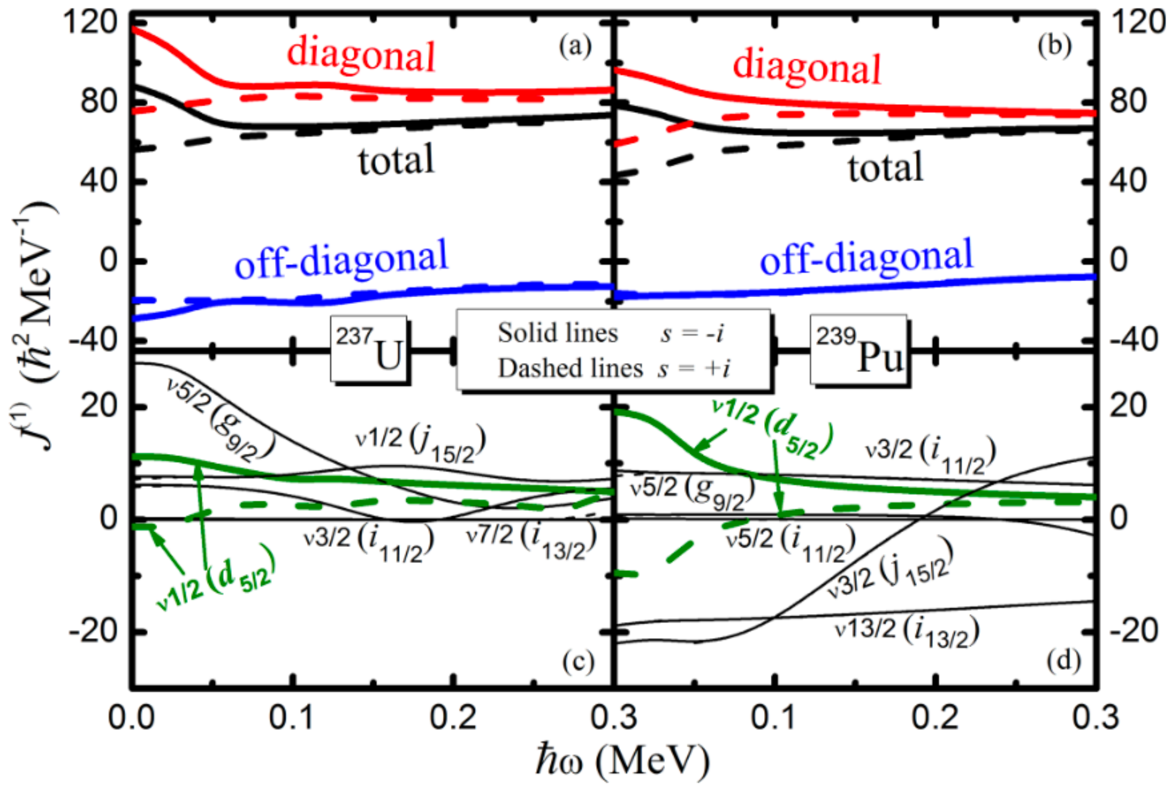


- $^{237}$U 和$^{239}$Pu为奇中子isotones (N=145),simplex splittings存在于中子体系中;
- simplex splitting主要由中子顺排的对角部分产生，主要产生于$\nu 1/2\ (d_{5/2})$轨道；

Jun Zhang, XTH*, Yu-Chun Li and Hai-Qian Zhang, PRC, 107, 024305 (2023).

# 4. Summary

# 4.1 summary

- **A new set of Nilsson parameters are proposed.**
- **A improved new set of Nilsson parameters are proposed.**

- **The experimental kinematic MoIs in even-even, odd-A, and odd-odd nuclei are all well reproduced by PNC-CSM.**
- **The proton N=7 shell (like the high-*j* intruder orbital $1j_{15/2}$) start to play an important role in the rotational properties.**

# 4.1 summary

- High-order deformation $\varepsilon_6$ is important.
- Reverse of the single-particle levels occur at N=153 in Lr isotopes which is due to the effect of the high-order deformation.
- High-K isomers (both of the excitation energies and the rotational bands build on it) can be described well.
- Pairing play an important role.
- $\varepsilon_3$ has been included in the PNC-CSM method.
- Octupole correlation influence strongly the rotational properties of U and Pu isotopes.

# Thank you !

Thank you !

# 3.7 Octupole deformation $\varepsilon_3$

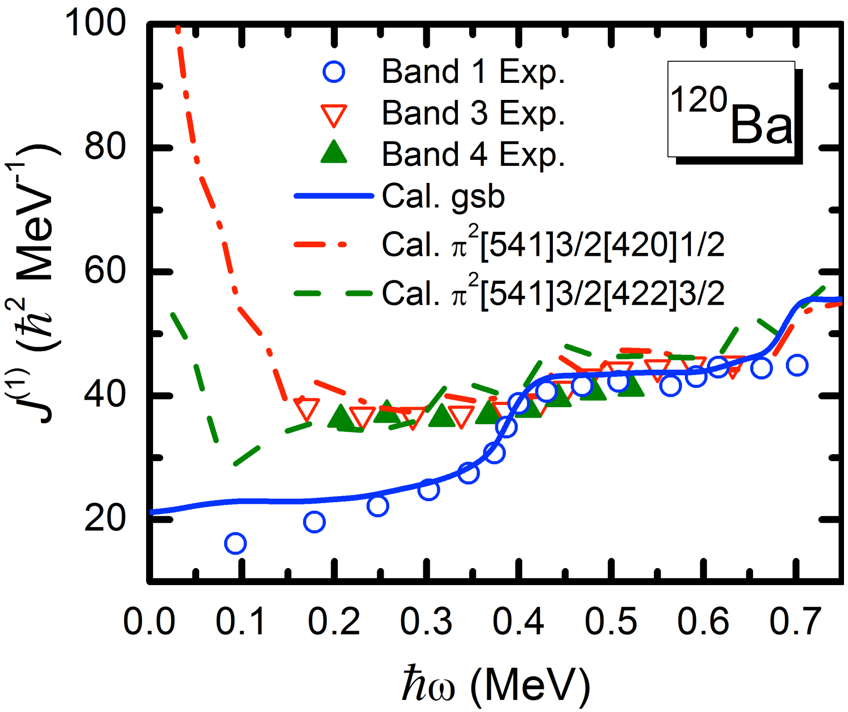


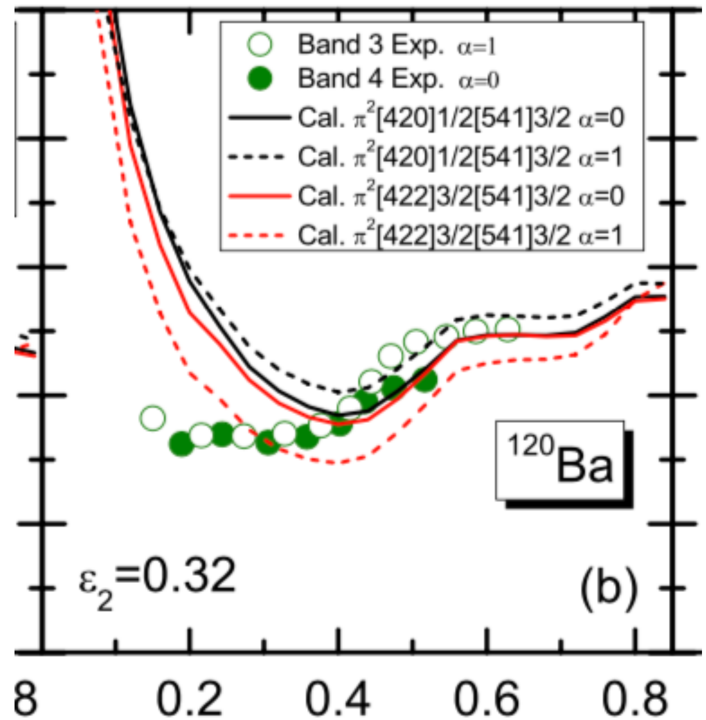


$$\varepsilon_2 = 0.32,\ \varepsilon_3 = 0.003$$

Octupole correlation in $^{120}$Ba

**B. F. Lv**, C. **M. Petrache**, K. K. Zheng, **Z. H. Zhang**, W. Sun, Z. P. Li, **X. T. He**, J. Zhang et al., Phys. Rev. C 105, 044319 (2022)